Oil Shale, 2020, Vol. 37, No. 1, pp. 1–31
doi: https://doi.org/10.3176/oil.2020.1.01
ISSN 0208-189X

Major, trace and rare earth element geochemistry of coal and oil shale in the Yuqia area, Middle Jurassic Shimengou Formation, northern Qaidam Basin

Yueyue Bai[(a)], Qingtian Lv[(a)*], Zhaojun Liu[(b)], Pingchang Sun[(b)], Yinbo Xu[(c)], Jingyao Meng[(d)], Qingtao Meng[(b)], Wenquan Xie[(b)], Junxian Wang[(b)], Kebing Wang[(b)]

[(a)] China Deep Exploration Center – SinoProbe Center, Chinese Academy of Geological Sciences, Beijing 100037, China
[(b)] Key Laboratory for Oil Shale and Coexisting Minerals Mineralization & Exploration and Exploitation, Jilin University, Changchun 130061, China
[(c)] Oil & Gas Survey, China Geological Survey, Beijing 100029, China
[(d)] Kansas Geological Survey, 1930 Constant Ave., Lawrence, KS 66047–3724, USA

Abstract. *Coal and oil shale in the Middle Jurassic Shimengou Formation of the northern Qaidam Basin (China) have been characterized and compared using total organic carbon (TOC) content, oil yield, and proximate as well as major, trace and rare earth element (REE) and X-ray powder diffraction (XRD) analyses.*

The results show that coal is represented by lignite and bituminous coal and oil shale is of medium quality. In both coal and oil shale, Si, Al, K, Ti and Na originate from a mixed clastic sedimentary component comprised of clay minerals, quartz and feldspars. In coal, rare earth elements (REEs) are related to phosphate minerals, whereas those in oil shale have inorganic affinities and are mainly associated with clay minerals and quartz. REEs in coal and oil shale are of terrigenous origin. Both coal and oil shale in the Yuqia area are possibly the products of source rocks that have experienced moderate chemical weathering during a warm and humid climate, and they have similar source rocks of felsic volcanic and sedimentary rocks.

Keywords: *Yuqia oil shale and coal, trace and rare earth elements, Middle Jurassic, Qaidam Basin.*

1. Introduction

Coal and oil shale are found to coexist in many basins in China, such as Huadian [1], Meihe [2], Fushun [3], Ordos [4], Huangxian [5], etc. On the

* Corresponding author: e-mail *yueying0210@126.com*

basis of occurrence and the size of reserves, a comprehensive exploration and development of these rocks can be carried out to improve the production efficiency, at the same time reducing the production costs. Many investigators have conducted a series of comparative studies on coexisting coal and oil shale [3, 6–8]. The characteristics of coal and oil shale depend on their contents of organic components (macerals) as well as minerals and other inorganic constituents (mineral matter) [9, 10]. The contents of some of the major and trace mineral–inorganic elements are closely related to the mineral content of clastic sedimentary rocks [11–16]. Rare earth elements (REEs) have the qualities of chemical stability, coherent behavior during different geochemical processes and predictable patterns of fractionation [17, 18]. As a result, trace and rare earth elements combined with major elements are widely used to study the paleoenvironment, paleoclimate, provenance and tectonic setting of clastic sedimentary rocks [19–23].

The Shimengou Formation in the Middle Jurassic Yuqia area is the main stratum of coexisting coal and oil shale. Some reseachers have studied coal [24, 25] and oil shale [26, 27] seams separately with respect to quality, modes of occurrence of formation, and metallogenic regularities, but studies of their inorganic geochemistry, provenance and tectonic setting are rare. This article aims to compare coal and oil shale in the Yuqia area, Middle Jurassic Shimengou Formation, in terms of quality, and analyze their inorganic geochemistry, e.g. the modes of occurrence of major, trace and rare earth elements, as well as as the provenance.

2. Geological setting

The Yuqia area is located in the central part of the northern Qaidam Basin in a long and narrow NE-trending zone. It is bordered by the Dakendaban Mountains in the north and east, and the Lvliang Mountains in the south (Fig. 1). The Lower Jurassic strata are missing in the Yuqia area.

The Upper Jurassic section consists of the Hongshuigou Formation and the Caishiling Formation. The Hongshuigou Formation is mostly composed of greyish-green and purplish-red siltstone and mudstone with fine sandstone interbedded. The Caishiling Formation is chiefly comprised of gray siltstone interbedded with conglomerate in the lower part.

The Middle Jurassic section consists of the Dameigou Formation and the Shimengou Formation. The former is primarily composed of gray sandy conglomerate, coarse-to-medium-grained sandstone and coal seams with abundant carbonaceous mudstone interbedded. The Shimengou Formation is the target layer, including the Coal-bearing Member and the Shale Member. Gray and black siltstone, mudstone and gray coarse-to-fine-grained sandstone are the main sediments and multilayered coal seams are found in the Coal-bearing Member. Black coals are filled with pyrite particles and the main

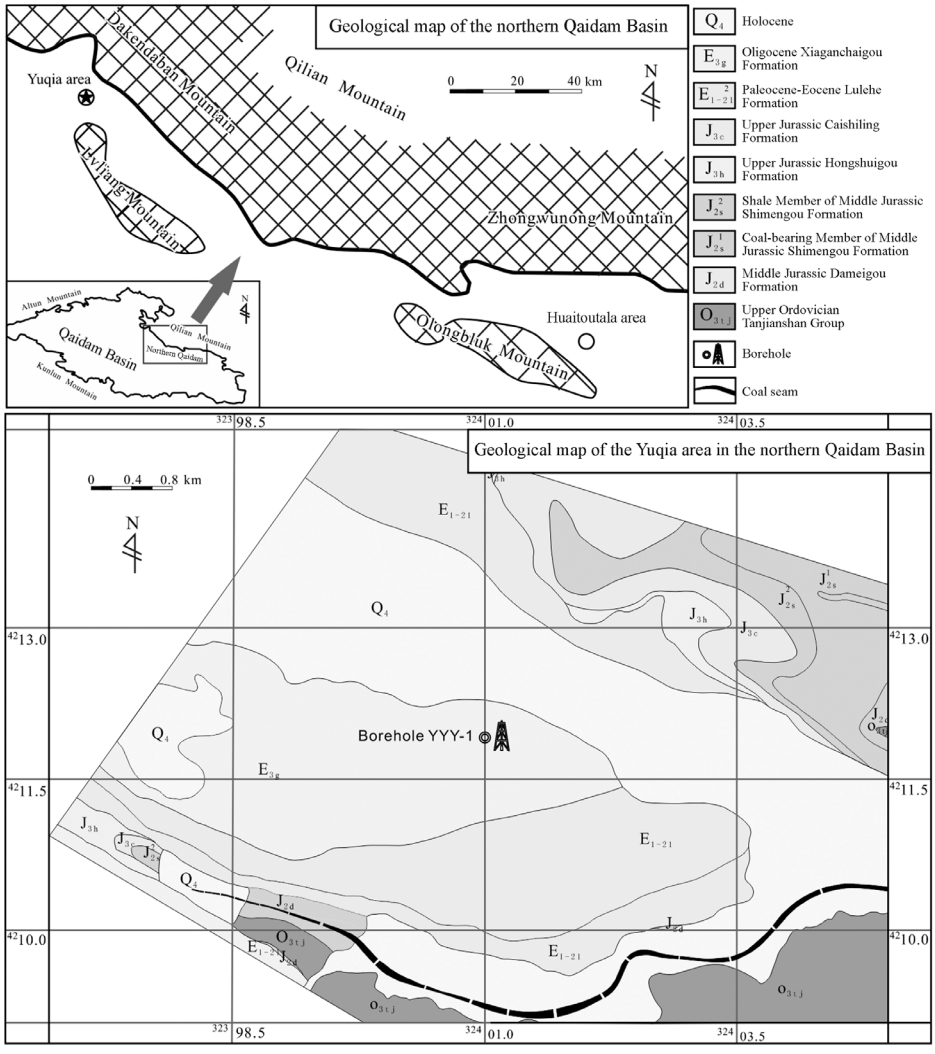

Fig. 1. Geological map of the Yuqia area in the Qaidam Basin.

depositional environments of the Coal-bearing Member are delta fronts and swamps. The Shale Member mainly consists of dark gray siltstone, mudstone and dark brown shale and oil shale. A shallow-to-deep lake is thought to be the main depositional environment. Large amounts of carbonate interlayers, siderite concretions, and ostracode and lamellibranch fossils are contained in oil shale. Laminations are highly developed in the Shale Member [24–28].

3. Materials and methods

Seven samples of coal from the Coal-bearing Member and twenty-three samples of oil shale from the Mudstone Member (Fig. 2) were collected to determine their total organic carbon (TOC) and total sulfur (TS) contents, trace, rare earth and major elements, and oil yield, as well as carry out proximate and X-ray powder diffraction (XRD) analyses.

3.1. Total organic carbon, total sulfur, oil yield and proximate analysis

The total organic carbon and total sulfur contents as well as oil yield were determined and proximate analysis (including moisture and volatile matter contents, ash yield, and calorific value) was performed in the Key Laboratory for Oil Shale and Coexisting Minerals Mineralization & Exploration and Exploitation, Changchun of Jilin Province, China. The TOC and TS contents were analysed using a LECO CS-230, following the Chinese standard GB/T 19145-2003 [29] and ASTM standard D3177-02 (2007) [30], respectively. Oil yield was determined using low-temperature carbonization furnaces, following the Chinese Petroleum Chemical Industry Standard SH/T 0508-92 [31]. The moisture and volatile matter contents, ash yield, and calorific values were determined following the ASTM standards D3173-11 (2011), D3175-11 (2011), D3174-11 (2011) and D5865-13 (2013) [32–35]. The moisture content was calculated after the samples had been heated at a temperature of 105 °C until constant mass. Ash yield and volatile matter content were both determined using a muffle furnace X1-2000. The volatile matter content was calculated by the reduced proportion minus water content after the samples had been heated in the absence of air. The calorific value was determined using a DC5015 calorimeter.

3.2. Major, trace and rare earth element analyses

Major, trace and rare earth elements were determined in the Analytical Laboratory of Beijing Research Institute of Uranium Geology. 25 to 50 mg samples were analyzed using the NexION300D inductively coupled plasma mass spectrometry (ICP-MS), following the technique described by Dai et al. [16]. Major elements contained in SiO_2, Al_2O_3, CaO, K_2O, Na_2O, Fe_2O_3, MnO, MgO, TiO_2 and P_2O_5 were identified using X-ray fluorescence (XRF) spectrometers AB104L, AL104 and AxiosmAX, following the analytical methods described by Kimura [36] and Dai et al. [16]. The analytical uncertainty was usually lower than 5%.

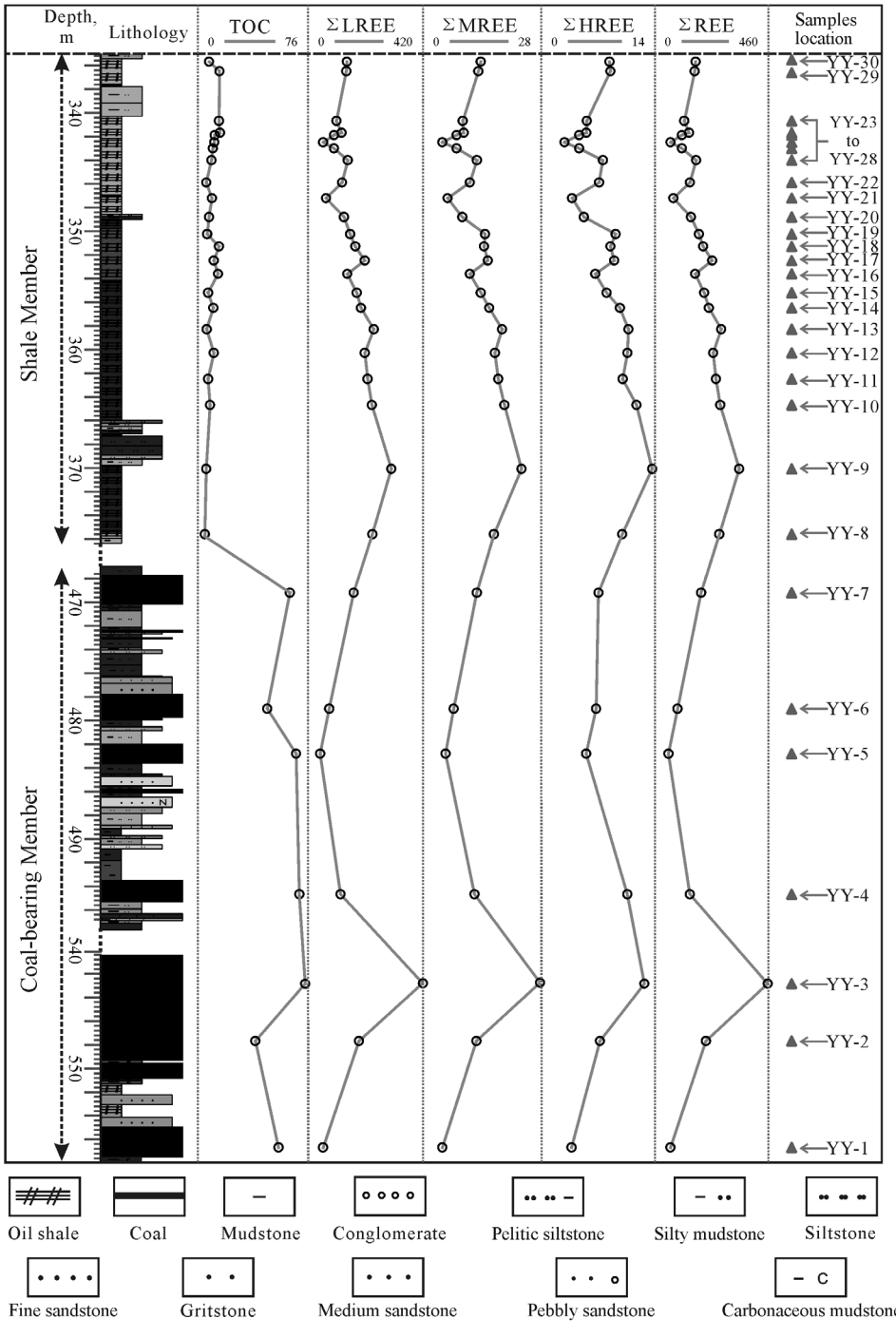

Fig. 2. Vertical distribution of REEs and samples location.

3.3. X-ray powder diffraction analysis

X-ray powder diffraction analysis was also performed in the Analytical Laboratory of Beijing Research Institute of Uranium Geology, following the method provided by Ward et al. [37, 38] and Ruan and Ward [39]. The Panalytical X'Pert PRO X-ray diffractometer was used to record X-ray spectrograms. Each mineral has a specific XRD pattern and the intensity of the characteristic peak in the spectrum positively correlates with the content of a mineral in the sample which can be determined through this relationship.

4. Results

4.1. Quality characterization of coal and oil shale

Coal in the Middle Jurassic Yuqia area can be classified into lignite and bituminous coal based on the Chinese national standard GB/T 5751-2009 [40]. The average content of TOC and TS are 60.00 wt% and 1.03%, respectively. The ash yield, water and volatile matter contents and calorific value are 30.81%, 3.84%, 35.64% and 19.43 MJ/kg, respectively (Table 1).

Oil shale in the Middle Jurassic Yuqia area has average TOC and TS contents of 9.21 wt% and 0.41%, respectively. Its oil yield is 6.43 wt%, ash yield 74.75%, water and volatile matter contents are 2.28% and 23.47%, respectively, and the calorific value is 4.25 MJ/kg (Table 1). The Yuqia area oil shale belongs to medium-quality oil shales [28].

4.2. Minerals in coal and oil shale

The mineralogical composition of coal samples from the Middle Jurassic Yuqia area comprises mainly clay minerals (29.2–76.4%) and quartz (10.2–30.6%). Some pyrite (3.6–26.6%), calcite (1.5–34%) and siderite (14.2%) can also be found in the coal samples. Kaolinite (52–100%) is the main component of clay minerals, and some samples also contain illite (25–36%) and an illite-smectite mixed layer (12–21%) (Table 2). The minerals in oil shale are chiefly clay minerals (25.5–72.1%), quartz (11.1–45%) and calcite (2.1–52.6%). In some oil shale samples aragonite may be quite abundant (15.9–51.6%), and some contain siderite (3.4–16.8%), plagioclase (5.6–8.5%) and dolomite (14.9%). The clay minerals in the the oil shale samples are primarily illite (14–52%), kaolinite (5–48%), an illite-smectite mixed layer (12–73%) and chlorite (4–11%), while in some samples smectite is present in high amounts, 56–75% (Table 2).

Table 1. TOC content, oil yield and proximate analysis of coal and oil shale in the Middle Jurassic Yuqia area of the Qaidam Basin

Sample No.	Lithology	TOC, wt%	TS, wt%	OY, wt%	A_{ad}, wt%	W_{ad}, wt%	V_{daf}, wt%	Q_{daf}, MJ/kg
YY-1	Coal	55.95	0.47	nd	42.94	2.96	30.42	16.20
YY-2	Coal	40.02	0.41	nd	35.02	4.68	37.46	18.30
YY-3	Coal	74.10	0.71	nd	21.60	4.46	44.40	29.33
YY-4	Coal	70.21	0.65	6.99	31.66	4.85	34.86	19.02
YY-5	Coal	67.90	1.80	nd	28.35	1.40	10.13	13.57
YY-6	Coal	48.10	2.37	9.30	29.63	3.86	59.32	18.80
YY-7	Coal	63.70	0.77	nd	26.48	4.67	32.87	20.80
Average		60.00	1.03	8.15	30.81	3.84	35.64	19.43
YY-8	Oil shale	4.15	0.19	4.02	83.54	1.59	14.77	1.87
YY-12	Oil shale	8.22	0.18	4.13	82.02	2.12	14.53	3.33
YY-13	Oil shale	6.41	0.12	4.35	84.14	2.59	13.26	2.39
YY-16	Oil shale	13.70	0.24	8.03	76.52	2.05	21.45	6.16
YY-18	Oil shale	8.85	0.22	4.67	81.00	2.76	15.62	3.56
YY-22	Oil shale	11.45	0.55	8.17	68.40	2.19	29.35	5.36
YY-24	Oil shale	10.70	0.16	9.17	62.90	1.96	35.18	4.69
YY-25	Oil shale	11.45	0.55	8.50	63.28	2.87	39.33	5.61
YY-27	Oil shale	15.35	1.49	10.20	70.75	3.74	27.55	7.31
YY-28	Oil shale	6.10	0.34	5.68	73.92	1.86	24.27	3.54
YY-30	Oil shale	4.97	0.46	3.79	75.74	1.38	22.84	2.92
Average		9.21	0.41	6.43	74.75	2.28	23.47	4.25

Note: nd denotes no data; TS denotes total sulfur; OY denotes oil yield; A denotes ash yield; W denotes moisture content; V denotes volatile matter; Q denotes calorific value; ad denotes air dried basis; daf denotes dry and ash-free basis.

Table 2. Minerals present in coal and oil shale samples collected from borehole YYY-1 in the Yuqia area, Qaidam Basin

Sample No.	Lithology	Relative content of minerals, [ω(B)/10^{-2}]				
		Quartz	Plagioclase	Calcite	Dolomite	Aragonite
YY-1	Coal	23.6	–	–	–	–
YY-2	Coal	–	–	–	–	–
YY-3	Coal	28.5	–	–	–	–
YY-4	Coal	10.2	–	34	–	–
YY-5	Coal	30.6	–	–	–	–
YY-6	Coal	–	–	–	–	–
YY-7	Coal	18.3	–	1.5	–	–
YY-8	Oil shale	30.7	–	–	–	–
YY-9	Oil shale	44.9	–	–	–	–
YY-10	Oil shale	27.9	–	–	–	–
YY-11	Oil shale	41.3	–	–	–	–
YY-12	Oil shale	38.9	–	–	–	–
YY-13	Oil shale	31.4	–	–	–	–
YY-14	Oil shale	37.4	–	–	–	–
YY-15	Oil shale	38.8	5.6	–	–	–
YY-16	Oil shale	43.1	8.5	–	–	–
YY-17	Oil shale	45	6.3	–	–	–
YY-18	Oil shale	31.8	–	13.8	–	–
YY-19	Oil shale	31.3	–	32.8	–	–
YY-20	Oil shale	41.4	–	–	–	–
YY-21	Oil shale	11.1	–	39	–	15.9
YY-22	Oil shale	14.4	–	52.6	–	–
YY-23	Oil shale	13.7	–	2.1	–	51.6
YY-24	Oil shale	13	–	18.8	14.9	27.8
YY-25	Oil shale	27.8	–	15.5	–	–
YY-26	Oil shale	18.2	–	19.2	–	–
YY-27	Oil shale	38.6	–	–	–	–
YY-28	Oil shale	14.9	–	39.8	–	–
YY-29	Oil shale	32.5	–	6.2	–	–
YY-30	Oil shale	16.8	–	37.5	–	–

Note: – denotes not determined.

Continuation of Table 2.

Relative content of minerals, [ω(B)/10^{-2}]			Relative content of clay minerals, [ω(B)/10^{-2}]				
Siderite	Pyrite	Clay minerals	Smectite	Illite/ smectite	Illite	Kaolinite	Chlorite
–	–	76.4	–	12	28	60	–
–	–	–	–	–	–	100	–
–	–	71.5	–	14	26	60	–
–	26.6	29.2	–	–	–	100	–
14.2	–	55.2	–	12	36	52	–
–	–	–	–	–	–	100	–
–	3.6	76.6	–	21	25	54	–
11.9	–	57.4	–	28	31	32	9
–	–	55.1	4	22	36	30	8
–	–	72.1	–	19	46	26	9
–	–	58.7	–	22	45	24	9
3.4	–	57.7	–	17	52	22	9
–	–	68.6	–	49	21	22	8
3.7	–	58.9	–	12	35	48	5
–	–	55.6	–	46	24	20	10
–	–	48.4	–	40	25	35	–
–	–	48.7	–	26	40	23	11
–	–	54.4	–	30	41	29	–
–	–	35.9	–	46	34	16	4
–	–	58.6	–	29	46	19	6
8.3	–	25.7	–	73	22	5	–
–	–	33	72	–	14	10	4
–	–	32.6	56	–	26	18	–
–	–	25.5	75	–	17	8	–
–	–	56.7	–	35	39	26	–
13.7	–	48.9	–	44	27	29	–
–	–	61.4	–	22	37	41	–
7.9	–	37.4	–	45	31	24	–
16.8	–	44.5	–	17	45	29	9
10.8	–	34.9	–	23	35	34	8

4.3. Rare earth element concentrations and normalized patterns

4.3.1. Rare earth element concentrations

A total of 14 rare earth elements (La, Ce, Pr, Nd, Sm, Eu, Gd, Tb, Dy, Ho, Er, Tm, Yb, Lu) were analyzed. They were classified into light REEs (LREEs – La, Ce, Pr, Nd, Sm), medium REEs (MREEs – Eu, Gd, Tb, Dy) and heavy REEs (HREEs – Ho, Er, Tm, Yb, Lu), based on the grouping by Seredin and Dai [17] and Dai et al. [18]. The total concentration of REEs (ΣREE) of Yuqia coal is 172.77 μg/g on average, which is higher than the respective average figure for Chinese coals (117.7 μg/g [41]), US coals (54 μg/g [42]) and coals worldwide (60 μg/g [43]). The total concentration of LREEs (ΣLREE) of Yuqia coal is 45.87–417.60 μg/g (average 153.27 μg/g), constituting about 89% of ΣREE. The concentration of HREEs (ΣHREE) is 3.75–12.72 μg/g (7.70 μg/g on average), making up only 4% of ΣREE, whereas the average concentration of MREEs (ΣMREE) is 11.80 μg/g (4.63–27.48 μg/g), accounting for about 7% of ΣREE.

The Shimengou Formation oil shale has an average REE concentration of 183.36 μg/g, which is higher than the upper continental crust (UCC) average 146.40 μg/g [44] and the North American Shale Composite (NASC) average 173.20 μg/g [45]). ΣLREE of Shimengou oil shale is 56.11–304.90 μg/g (average 162.19 μg/g) and makes up 88% of ΣREE, being higher than the average for Chinese oil shales (61.48 μg/g [46]) and Australian oil shales (63.00 μg/g [47]). ΣHREE is 2.88–13.69 μg/g (average 7.93 μg/g) and makes up only 4% of ΣREE, which is also higher than Chinese oil shales average (6.71 μg/g [46]) but lower than Australian oil shales average (14.40 μg/g [47]). The total average concentration of MREEs (ΣMREE) of Shimengou oil shale, 13.24 μg/g (4.70–23.34 μg/g), is similar to that of coal, and also forms about 7% of ΣREE.

4.3.2. Chondrite-normalized patterns

REE abundances in coal and oil shale are normalized to chondrite (Fig. 3) and similar distribution trends are displayed for all samples. The average ratios of ΣLREE/ΣHREE (L/H) for coal and oil shale are 19.91 and 20.45, respectively, showing LREE enrichment and HREE deficit [48, 49]. The average values of $(La/Yb)_N$, $(Ce/Yb)_N$, $(La/Sm)_N$ and $(Gd/Yb)_N$ for coal are 8.12, 5.65, 4.59 and 1.25, respectively, and for oil shale 8.31, 6.07, 3.92 and 1.43, respectively. All these values are in agreement with LREE enrichment and HREE deficit figures given above. For comparison, LREEs in oil shale are more enriched than in coal [17].

All the chondrite-normalized patterns have shown a certain degree of negative Eu anomaly and negligible Ce anomaly (the average values of Eu/EuN* for coal and oil shale are 0.60 and 0.67, respectively, and Ce/CeN* are 0.94 and 0.96, respectively ([48]; Table 3; Fig. 3). Compared with oil shale, coal has shown a higher degree of Ce abnormality.

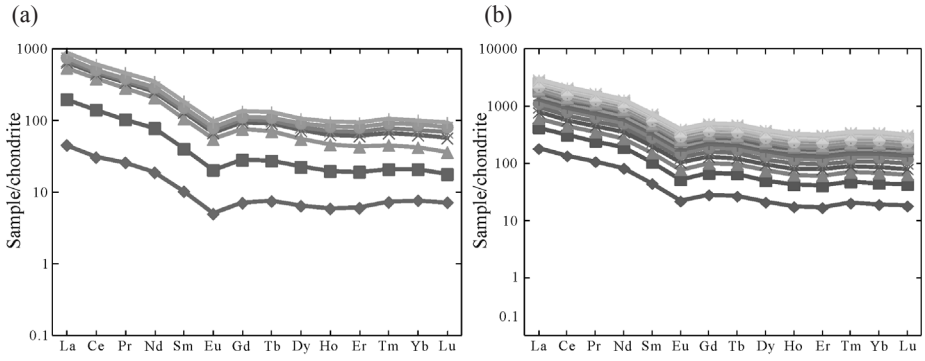

Fig. 3. Chondrite-normalized patterns for: a) coal, b) oil shale.

5. Discussion

5.1. Modes of occurrence of major elements

5.1.1. Modes of occurrence of major elements in coal

SiO_2, Al_2O_3, K_2O, MgO, TiO_2 and Na_2O in coal are highly correlated with ash yield (the coefficients are 0.72–0.84) and between themselves (Table 4). The major elements Si, Al, Mg, K, Ti and Na are related to detrital minerals such as quartz and clays [51–53], indicating that they originate from a mixed clay assemblage.

SiO_2, K_2O and Al_2O_3 have a very strong positive correlation with ash yield ($R^2 \geq 0.72$) (Table 4). Si is mostly contained in quartz and aluminosilicate minerals, which are the major components of ash [36, 54]. Al_2O_3 is present in aluminosilicate minerals, and K_2O is related to illite, which is contained in K-bearing clay minerals in the form of interlayer cations [36, 55]. The strong correlation of these compounds with ash yield indicate the enrichment of clay minerals and quartz in the samples. Most samples have relatively low ratios of Al_2O_3/SiO_2 (0.44–0.60; Table 5), suggesting the quartz source of Si besides clay minerals [2, 53]. These values agree with the amounts of quartz, kaolinite, illite and an illite-smectite mixed layer determined by XRD in coal (Table 2).

Mg might be related to carbonate minerals or Mg-bearing clay minerals (via illite and an illite-smectite mixed layer and montmorillonite [36, 56]). In the Yuqia area, MgO in coal has exhibited a high positive correlation with ash yield (0.79), indicating its possible relation to illite and an illite-smectite mixed layer (Table 2). Ti mainly occurs in titanium oxide and is correlated with organic matter and clay minerals [57–59]. The correlation coefficients of 0.90 for TiO_2-Al_2O_3, 0.78 for TiO_2-ash yield and 0.55 for TiO_2-TOC give evidence of the strong positive relationship between the components. Na is mostly present in alkali feldspar or clay minerals other than in porewater

Table 3. Rare earth element concentrations of Yuqia coal and oil shale, μg/g

Sample No.	Lithology	La	Ce	Pr	Nd	Sm	Eu	Gd	Tb	Dy	Ho	Er	Tm	Yb	Lu
YY-1	Coal	14.10	24.80	3.11	11.30	2.04	0.37	1.84	0.35	2.07	0.43	1.26	0.23	1.60	0.23
YY-2	Coal	46.90	89.70	9.35	35.70	6.03	1.14	5.50	0.94	5.16	0.99	2.77	0.44	2.75	0.34
YY-3	Coal	108.00	196.00	21.80	78.60	13.20	2.55	12.50	2.03	10.40	1.91	4.98	0.79	4.46	0.58
YY-4	Coal	33.40	49.10	6.43	25.70	4.75	0.93	4.76	0.92	5.64	1.25	3.72	0.69	4.33	0.66
YY-5	Coal	9.64	21.70	2.53	9.92	2.08	0.38	1.93	0.41	2.67	0.60	1.86	0.36	2.39	0.38
YY-6	Coal	24.20	34.60	3.62	13.80	2.55	0.52	2.62	0.54	3.61	0.79	2.36	0.44	2.80	0.41
YY-7	Coal	38.10	78.20	9.41	35.90	6.62	1.16	5.74	0.98	4.93	0.92	2.56	0.45	2.75	0.41
Average		39.19	70.59	8.04	30.13	5.32	1.01	4.98	0.88	4.93	0.98	2.79	0.49	3.01	0.43
YY-8	Oil shale	56.00	109.00	12.80	48.90	8.85	1.61	7.30	1.25	6.71	1.25	3.53	0.65	3.98	0.57
YY-9	Oil shale	73.00	141.00	16.20	62.90	11.80	2.20	10.00	1.79	9.35	1.78	4.93	0.86	5.32	0.80
YY-10	Oil shale	57.70	105.00	12.80	49.70	9.27	1.87	8.23	1.42	7.82	1.45	4.27	0.70	4.69	0.64
YY-11	Oil shale	53.10	98.90	12.00	46.60	8.79	1.78	7.82	1.27	6.98	1.27	3.64	0.59	4.04	0.53
YY-12	Oil shale	51.60	93.50	11.30	44.00	8.43	1.68	7.43	1.22	6.80	1.30	3.76	0.63	4.37	0.60
YY-13	Oil shale	59.10	109.00	13.00	49.80	9.56	1.78	8.16	1.41	7.41	1.40	3.85	0.67	4.23	0.63
YY-14	Oil shale	47.70	88.90	10.40	39.80	7.49	1.47	6.72	1.14	6.36	1.20	3.48	0.59	3.92	0.55
YY-15	Oil shale	42.80	80.60	9.67	38.00	7.02	1.30	6.04	1.03	5.37	1.02	2.88	0.51	3.20	0.47
YY-16	Oil shale	35.30	66.40	7.71	30.10	5.63	1.13	4.76	0.82	4.44	0.88	2.38	0.42	2.63	0.40
YY-17	Oil shale	52.20	95.60	11.20	42.40	7.71	1.61	6.76	1.10	5.95	1.06	3.18	0.54	3.76	0.49
YY-18	Oil shale	40.60	80.30	9.34	35.90	6.89	1.51	6.12	1.04	5.79	1.10	3.14	0.51	3.36	0.43
YY-19	Oil shale	36.00	70.40	8.54	33.90	6.61	1.36	5.91	1.10	6.34	1.20	3.28	0.60	3.61	0.52
YY-20	Oil shale	31.80	59.70	7.33	28.10	5.04	0.97	4.12	0.68	3.54	0.65	1.84	0.32	2.15	0.31
YY-21	Oil shale	16.20	30.00	3.47	13.60	2.57	0.61	2.37	0.42	2.44	0.48	1.41	0.22	1.50	0.20
YY-22	Oil shale	30.00	57.70	6.50	25.80	4.99	1.04	4.53	0.82	4.78	0.95	2.59	0.45	2.76	0.38
YY-23	Oil shale	33.40	68.10	7.75	31.40	5.98	1.29	5.35	0.96	5.18	1.01	2.76	0.49	2.93	0.43
YY-24	Oil shale	21.90	46.40	5.02	19.60	3.71	0.81	3.34	0.59	3.28	0.61	1.71	0.28	1.82	0.27
YY-25	Oil shale	13.50	26.10	2.95	11.40	2.16	0.46	1.96	0.37	1.91	0.38	1.02	0.18	1.15	0.15
YY-26	Oil shale	23.50	44.00	5.23	20.20	3.82	0.75	3.41	0.61	3.22	0.63	1.69	0.29	1.82	0.27
YY-27	Oil shale	29.60	56.50	6.81	26.30	4.95	0.97	4.25	0.72	3.79	0.72	2.03	0.35	2.17	0.31
YY-28	Oil shale	25.50	48.00	5.56	21.40	4.15	0.87	3.78	0.67	4.18	0.72	2.00	0.33	2.28	0.30
YY-29	Oil shale	33.30	64.70	7.51	29.60	5.98	1.26	5.27	0.95	5.69	1.07	3.42	0.47	3.20	0.41
YY-30	Oil shale	32.90	65.60	7.76	30.50	5.97	1.32	5.52	1.00	5.92	1.10	3.09	0.51	3.33	0.43
Average		38.99	74.15	8.73	33.91	6.41	1.29	5.62	0.97	5.36	1.01	2.86	0.48	3.14	0.44
Chondrite		0.31	0.81	0.12	0.60	0.20	0.07	0.26	0.05	0.32	0.07	0.21	0.03	0.21	0.03

Note: ΣLREE – total content of light rare earth elements (ΣLREE = La + Ce + Pr + Nd + Sm); ΣMREE – total content of medium rare earth elements (ΣMREE = Eu + Gd + Tb + Dy); ΣHREE – total content of heavy rare earth elements (ΣHREE = Ho + Er + Tm + Yb + Lu); ΣREE – total content of rare earth elements (ΣREE = ΣLREE + ΣMREE + ΣHREE); L/H = ΣLREE/ΣHREE; N – chondrite-normalized; $Eu/Eu^*_N = Eu_N/(Sm_N \times Gd_N)^{1/2}$, Eu_N, Sm_N and Gd_N represent the chondrite-normalized value; $Ce/Ce^*_N = Ce_N/(La_N \times Pr_N)^{1/2}$, Ce_N, La_N and Pr_N represent the chondrite-normalized value [50]. Data source: Chondrite [45].

Continuation of Table 3.

ΣLREE	ΣMREE	ΣHREE	ΣREE	L/H	(La/Lu)N	(La/Yb)N	(Ce/Yb)N	(La/Sm)N	(Gd/Yb)N	Eu/EuN*	Ce/CeN*
55.35	4.63	3.75	63.73	14.76	5.93	5.94	4.00	4.46	0.92	0.59	0.89
187.68	12.74	7.29	207.71	25.74	13.35	11.50	8.42	5.02	1.61	0.61	1.02
417.6	27.48	12.72	457.8	32.83	18.02	16.33	11.34	5.28	2.25	0.61	0.96
119.38	12.25	10.65	142.28	11.21	4.90	5.20	2.93	4.54	0.88	0.60	0.80
45.87	5.39	5.59	56.85	8.21	2.46	2.72	2.34	2.99	0.65	0.59	1.05
78.77	7.29	6.8	92.86	11.58	5.71	5.83	3.19	6.12	0.75	0.62	0.88
168.23	12.81	7.09	188.13	23.73	8.99	9.34	7.34	3.71	1.68	0.58	0.98
153.27	11.8	7.7	172.77	19.91	8.48	8.12	5.65	4.59	1.25	0.60	0.94
235.55	16.87	9.98	262.4	23.60	9.51	9.49	7.07	4.08	1.47	0.62	0.97
304.9	23.34	13.69	341.93	22.27	8.83	9.25	6.84	3.99	1.51	0.62	0.98
234.47	19.34	11.75	265.56	19.95	8.72	8.29	5.78	4.02	1.41	0.66	0.92
219.39	17.85	10.07	247.31	21.79	9.70	8.86	6.32	3.90	1.56	0.66	0.93
208.83	17.13	10.66	236.62	19.59	8.32	7.96	5.52	3.95	1.37	0.65	0.92
240.46	18.76	10.78	270	22.31	9.08	9.42	6.65	3.99	1.55	0.62	0.94
194.29	15.69	9.74	219.72	19.95	8.39	8.20	5.85	4.11	1.38	0.64	0.95
178.09	13.74	8.08	199.91	22.04	8.81	9.02	6.50	3.93	1.52	0.62	0.94
145.14	11.15	6.71	163	21.63	8.54	9.05	6.51	4.05	1.45	0.67	0.96
209.11	15.42	9.03	233.56	23.16	10.31	9.36	6.56	4.37	1.45	0.69	0.94
173.03	14.46	8.54	196.03	20.26	9.14	8.15	6.17	3.80	1.46	0.72	0.98
155.45	14.71	9.21	179.37	16.88	6.70	6.72	5.03	3.51	1.32	0.67	0.96
131.97	9.31	5.27	146.55	25.04	9.93	9.97	7.16	4.07	1.54	0.66	0.93
65.84	5.84	3.81	75.49	17.28	7.84	7.28	5.16	4.07	1.27	0.77	0.95
124.99	11.17	7.13	143.29	17.53	7.64	7.33	5.39	3.88	1.32	0.67	0.98
146.63	12.78	7.62	167.03	19.24	7.52	7.69	6.00	3.60	1.47	0.70	1.01
96.63	8.02	4.69	109.34	20.60	7.85	8.11	6.58	3.81	1.48	0.71	1.05
56.11	4.7	2.88	63.69	19.48	8.71	7.91	5.86	4.03	1.37	0.69	0.98
96.75	7.99	4.7	109.44	20.59	8.42	8.71	6.24	3.97	1.51	0.64	0.95
124.16	9.73	5.58	139.47	22.25	9.24	9.20	6.72	3.86	1.57	0.65	0.95
104.61	9.5	5.63	119.74	18.58	8.23	7.54	5.43	3.96	1.33	0.67	0.96
141.09	13.17	8.57	162.83	16.46	7.86	7.02	5.22	3.59	1.32	0.69	0.97
142.73	13.76	8.46	164.95	16.87	7.40	6.66	5.08	3.56	1.33	0.71	0.98
162.19	13.24	7.93	183.36	20.45	8.55	8.31	6.07	3.92	1.43	0.67	0.96
2.04	0.7	0.55	3.29	3.71	1.00	1.00	1.00	1.03	1.00	1.01	0.99

Table 4. The correlation coefficients (R^2) between ΣREE, total sulfur, TOC, and major and rare earth elements of Yuqia coal

	TOC	S^T	Ash	SiO_2	Al_2O_3	Fe^T	MgO	CaO	Na_2O	K_2O	MnO	Ti_2O	P_2O_5	ΣREE	Th	U	Li	Be	Sc	V	Cr
TOC	1.00	□	□	□	□	□	□	□	□	□	□	□	□	□	□	□	□	□	□	□	□
S^T	–0.18	1.00	□	□	□	□	□	□	□	□	□	□	□	□	□	□	□	□	□	□	□
Ash	0.14	–0.34	1.00	□	□	□	□	□	□	□	□	□	□	□	□	□	□	□	□	□	□
SiO_2	0.49	–0.57	0.81	1.00	□	□	□	□	□	□	□	□	□	□	□	□	□	□	□	□	□
Al_2O_3	0.27	–0.36	0.72	0.91	1.00	□	□	□	□	□	□	□	□	□	□	□	□	□	□	□	□
Fe^T	–0.51	0.84	–0.26	–0.65	–0.44	1.00	□	□	□	□	□	□	□	□	□	□	□	□	□	□	□
MgO	0.51	–0.56	0.79	1.00	0.92	–0.65	1.00	□	□	□	□	□	□	□	□	□	□	□	□	□	□
CaO	–0.06	0.96	–0.14	–0.42	–0.27	0.86	–0.41	1.00	□	□	□	□	□	□	□	□	□	□	□	□	□
Na_2O	0.59	–0.69	0.74	0.97	0.81	–0.78	0.97	–0.54	1.00	□	□	□	□	□	□	□	□	□	□	□	□
K_2O	0.45	–0.56	0.84	1.00	0.91	–0.63	0.99	–0.42	0.97	1.00	□	□	□	□	□	□	□	□	□	□	□
MnO	–0.16	0.98	–0.20	–0.46	–0.26	0.90	–0.46	0.98	–0.61	–0.46	1.00	□	□	□	□	□	□	□	□	□	□
Ti_2O	0.55	–0.57	0.78	1.00	0.90	–0.68	1.00	–0.42	0.98	0.99	–0.47	1.00	□	□	□	□	□	□	□	□	□
P_2O_5	–0.74	0.34	–0.49	–0.56	–0.24	0.44	–0.56	0.19	–0.67	–0.57	0.32	–0.57	1.00	□	□	□	□	□	□	□	□
ΣREE	–0.36	0.49	–0.55	–0.38	–0.01	0.43	–0.35	0.29	–0.51	–0.40	0.42	–0.38	0.72	1.00□	□	□	□	□	□	□	□
Th	–0.04	0.17	–0.24	0.11	0.44	0.01	0.14	0.05	–0.02	0.07	0.16	0.12	0.53	0.84	1.00	□	□	□	□	□	□
U	–0.20	0.26	–0.10	0.13	0.50	0.18	0.15	0.14	–0.04	0.11	0.26	0.12	0.51	0.86	0.95	1.00	□	□	□	□	□
Li	0.65	–0.56	0.63	0.95	0.84	–0.70	0.95	–0.46	0.96	0.94	–0.51	0.95	–0.67	–0.30	0.15	0.14	1.00	□	□	□	□
Be	–0.26	–0.60	0.46	0.25	0.12	–0.39	0.22	–0.46	0.29	0.27	–0.49	0.25	0.05	–0.60	–0.41	–0.45	0.01	1.00	□	□	□
Sc	–0.20	–0.39	0.59	0.54	0.64	–0.32	0.53	–0.27	0.45	0.54	–0.24	0.54	0.26	–0.11	0.25	0.24	0.28	0.71	1.00	□	□
V	0.02	–0.63	0.69	0.73	0.72	–0.58	0.72	–0.49	0.68	0.73	–0.49	0.73	–0.02	–0.32	0.12	0.09	0.51	0.75	0.95	1.00	□
Cr	0.44	–0.33	0.30	0.74	0.86	–0.55	0.77	–0.31	0.67	0.70	–0.27	0.76	–0.08	0.25	0.72	0.64	0.76	–0.09	0.50	0.57	1.00
Co	–0.06	0.61	0.19	–0.19	–0.15	0.56	–0.20	0.77	–0.28	–0.18	0.72	–0.18	0.15	–0.16	–0.21	–0.18	–0.39	0.17	0.22	0.03	–0.29
Ni	0.07	–0.25	0.87	0.70	0.69	–0.22	0.68	–0.04	0.60	0.71	–0.08	0.69	–0.16	–0.43	–0.06	0.00	0.44	0.63	0.85	0.85	0.39
Cu	–0.22	0.02	–0.44	–0.08	0.22	–0.04	–0.05	–0.20	–0.14	–0.10	–0.06	–0.08	0.54	0.87	0.89	0.85	0.04	–0.45	0.01	–0.07	0.51
Zn	–0.12	–0.19	0.21	0.04	–0.01	–0.15	0.03	–0.03	0.04	0.03	–0.06	0.07	0.26	–0.38	–0.20	–0.32	–0.21	0.81	0.69	0.61	–0.04
Ga	0.46	–0.37	0.93	0.93	0.80	–0.41	0.91	–0.18	0.88	0.94	–0.25	0.91	–0.69	–0.53	–0.15	–0.05	0.84	0.23	0.42	0.59	0.49
Rb	0.62	–0.48	0.64	0.90	0.77	–0.60	0.90	–0.39	0.91	0.90	–0.45	0.89	–0.75	–0.32	0.05	0.10	0.97	–0.09	0.13	0.37	0.63
Sr	–0.47	0.58	–0.43	–0.37	0.03	0.55	–0.35	0.40	–0.53	–0.38	0.53	–0.39	0.76	0.98	0.80	0.87	–0.35	–0.53	–0.02	–0.27	0.19
Mo	–0.60	0.13	0.23	0.12	0.42	0.31	0.12	0.00	–0.05	0.16	0.11	0.05	0.38	0.55	0.47	0.70	0.06	–0.18	0.22	0.10	0.21
Cd	–0.70	–0.46	0.33	0.19	0.32	–0.14	0.17	–0.54	0.13	0.23	–0.45	0.13	0.35	0.09	0.11	0.25	0.05	0.49	0.52	0.50	0.08
In	0.45	–0.45	0.58	0.90	0.92	–0.57	0.91	–0.41	0.85	0.89	–0.41	0.89	–0.44	–0.01	0.41	0.44	0.95	–0.11	0.33	0.50	0.85
Sb	0.15	–0.67	0.91	0.83	0.68	–0.57	0.81	–0.49	0.83	0.85	–0.55	0.81	–0.46	–0.67	–0.29	–0.23	0.66	0.70	0.69	0.85	0.35
Cs	0.65	–0.47	0.61	0.89	0.77	–0.60	0.90	–0.38	0.90	0.89	–0.44	0.88	–0.75	–0.30	0.08	0.12	0.98	–0.13	0.11	0.35	0.66
Ba	–0.49	0.57	–0.38	–0.34	0.07	0.56	–0.31	0.40	–0.51	–0.34	0.53	–0.35	0.75	0.97	0.80	0.88	–0.33	–0.51	0.01	–0.24	0.21
W	–0.33	–0.02	–0.36	–0.57	–0.73	0.21	–0.59	–0.13	–0.45	–0.54	–0.14	–0.60	–0.11	–0.19	–0.62	–0.54	–0.46	–0.07	–0.67	–0.61	–0.81
Tl	–0.28	0.58	–0.06	–0.57	–0.66	0.72	–0.59	0.64	–0.57	–0.53	0.58	–0.60	–0.05	–0.28	–0.68	–0.55	–0.64	–0.02	–0.42	–0.53	–0.89
Pb	0.41	–0.48	0.31	0.76	0.85	–0.65	0.79	–0.47	0.72	0.73	–0.43	0.78	–0.12	0.20	0.67	0.59	0.80	–0.04	0.48	0.59	0.98
Bi	0.40	–0.55	0.11	0.63	0.68	–0.70	0.65	–0.61	0.64	0.60	–0.57	0.64	–0.18	0.24	0.60	0.52	0.76	–0.19	0.20	0.36	0.86
Nb	0.54	–0.50	0.80	0.97	0.85	–0.58	0.97	–0.36	0.95	0.97	–0.42	0.96	–0.71	–0.41	0.01	0.06	0.96	0.10	0.34	0.55	0.64
Ta	0.65	–0.33	0.55	0.86	0.80	–0.50	0.87	–0.26	0.84	0.85	–0.30	0.86	–0.66	–0.13	0.25	0.28	0.96	–0.26	0.10	0.30	0.74
Zr	0.47	–0.63	0.84	0.97	0.83	–0.69	0.96	–0.44	0.96	0.97	–0.50	0.97	–0.56	–0.54	–0.04	–0.05	0.87	0.45	0.63	0.82	0.64
Hf	0.55	–0.55	0.80	1.00	0.89	–0.65	1.00	–0.41	0.98	0.99	–0.46	0.99	–0.63	–0.40	0.07	0.09	0.97	0.20	0.46	0.67	0.72

Note: Fe^T represents total Fe.

Continuation of Table 4.

Co	Ni	Cu	Zn	Ga	Rb	Sr	Mo	Cd	In	Sb	Cs	Ba	W	Tl	Pb	Bi	Nb	Ta	Zr	Hf
□	□	□	□	□	□	□	□	□	□	□	□	□	□	□	□	□	□	□	□	□
□	□	□	□	□	□	□	□	□	□	□	□	□	□	□	□	□	□	□	□	□
□	□	□	□	□	□	□	□	□	□	□	□	□	□	□	□	□	□	□	□	□
□	□	□	□	□	□	□	□	□	□	□	□	□	□	□	□	□	□	□	□	□
□	□	□	□	□	□	□	□	□	□	□	□	□	□	□	□	□	□	□	□	□
□	□	□	□	□	□	□	□	□	□	□	□	□	□	□	□	□	□	□	□	□
□	□	□	□	□	□	□	□	□	□	□	□	□	□	□	□	□	□	□	□	□
□	□	□	□	□	□	□	□	□	□	□	□	□	□	□	□	□	□	□	□	□
□	□	□	□	□	□	□	□	□	□	□	□	□	□	□	□	□	□	□	□	□
□	□	□	□	□	□	□	□	□	□	□	□	□	□	□	□	□	□	□	□	□
□	□	□	□	□	□	□	□	□	□	□	□	□	□	□	□	□	□	□	□	□
□	□	□	□	□	□	□	□	□	□	□	□	□	□	□	□	□	□	□	□	□
□	□	□	□	□	□	□	□	□	□	□	□	□	□	□	□	□	□	□	□	□
□	□	□	□	□	□	□	□	□	□	□	□	□	□	□	□	□	□	□	□	□
□	□	□	□	□	□	□	□	□	□	□	□	□	□	□	□	□	□	□	□	□
□	□	□	□	□	□	□	□	□	□	□	□	□	□	□	□	□	□	□	□	□
□	□	□	□	□	□	□	□	□	□	□	□	□	□	□	□	□	□	□	□	□
□	□	□	□	□	□	□	□	□	□	□	□	□	□	□	□	□	□	□	□	□
□	□	□	□	□	□	□	□	□	□	□	□	□	□	□	□	□	□	□	□	□
□	□	□	□	□	□	□	□	□	□	□	□	□	□	□	□	□	□	□	□	□
□	□	□	□	□	□	□	□	□	□	□	□	□	□	□	□	□	□	□	□	□
1.00	□	□	□	□	□	□	□	□	□	□	□	□	□	□	□	□	□	□	□	□
0.45	1.00	□	□	□	□	□	□	□	□	□	□	□	□	□	□	□	□	□	□	□
–0.56	–0.39	1.00	□	□	□	□	□	□	□	□	□	□	□	□	□	□	□	□	□	□
0.57	0.60	–0.43	1.00	□	□	□	□	□	□	□	□	□	□	□	□	□	□	□	□	□
0.05	0.75	–0.36	0.02	1.00	□	□	□	□	□	□	□	□	□	□	□	□	□	□	□	□
–0.41	0.36	–0.01	–0.37	0.86	1.00	□	□	□	□	□	□	□	□	□	□	□	□	□	□	□
–0.01	–0.29	0.78	–0.30	–0.47	–0.36	1.00	□	□	□	□	□	□	□	□	□	□	□	□	□	□
–0.25	0.09	0.55	–0.41	0.11	0.13	0.64	1.00	□	□	□	□	□	□	□	□	□	□	□	□	□
–0.38	0.26	0.29	0.06	0.10	0.04	0.16	0.71	1.00	□	□	□	□	□	□	□	□	□	□	□	□
–0.45	0.40	0.31	–0.32	0.76	0.92	–0.05	0.35	0.21	1.00	□	□	□	□	□	□	□	□	□	□	□
–0.01	0.83	–0.41	0.38	0.84	0.62	–0.60	0.06	0.43	0.56	1.00	□	□	□	□	□	□	□	□	□	□
–0.41	0.34	0.01	–0.38	0.84	1.00	–0.35	0.11	0.00	0.92	0.58	1.00	□	□	□	□	□	□	□	□	□
0.00	–0.25	0.77	–0.30	–0.43	–0.34	1.00	0.67	0.19	–0.02	–0.56	–0.32	1.00	□	□	□	□	□	□	□	□
–0.31	–0.64	–0.21	–0.36	–0.44	–0.31	–0.22	–0.06	0.11	–0.53	–0.31	–0.33	–0.24	1.00	□	□	□	□	□	□	□
0.61	–0.13	–0.66	0.07	–0.22	–0.50	–0.16	–0.19	–0.27	–0.73	–0.26	–0.52	–0.16	0.54	1.00	□	□	□	□	□	□
–0.44	0.34	0.53	–0.09	0.49	0.68	0.13	0.24	0.19	0.88	0.40	0.70	0.14	–0.71	–0.94	1.00	□	□	□	□	□
–0.73	0.02	0.64	–0.36	0.33	0.69	0.11	0.24	0.20	0.84	0.24	0.71	0.11	–0.41	–0.94	0.93	1.00	□	□	□	□
–0.24	0.58	–0.13	–0.16	0.95	0.97	–0.41	0.14	0.12	0.90	0.77	0.96	–0.37	–0.42	–0.46	0.67	0.59	1.00	□	□	□
–0.37	0.31	0.13	–0.43	0.79	0.97	–0.18	0.17	–0.06	0.95	0.47	0.98	–0.15	–0.43	–0.56	0.75	0.74	0.92	1.00	□	□
–0.07	0.79	–0.24	0.26	0.91	0.80	–0.52	–0.03	0.18	0.77	0.91	0.79	–0.48	–0.56	–0.49	0.67	0.50	0.91	0.73	1.00	□
–0.21	0.65	–0.10	–0.02	0.93	0.93	–0.40	0.09	0.13	0.90	0.81	0.92	–0.37	–0.53	–0.54	0.74	0.63	0.98	0.89	0.96	1.00

[2, 36, 53]. Na_2O in coal has a relatively strong positive correlation with ash yield, SiO_2, Al_2O_3, K_2O, MgO and TiO_2 ($R^2 \geq 0.74$) (Table 4), indicating the existence of Na-bearing clay minerals and an illite-smectite mixed layer or minor alkali feldspar. In addition, the TOC content in coal is also positively correlated with SiO_2, MgO, Na_2O, K_2O and Ti_2O (0.45–0.59; Table 4), giving evidence of that clay minerals in coal have some affinity for organic matter. The above results suggest the dominance of clay minerals in the inorganic fraction of coal samples.

Fe is chiefly present in siderite, pyrite, ferrous sulfate and iron oxide, and it is commonly related to pyrite in high-sulfur coal [36, 60]. This is also the case with the coal of the studied area. The TS content in coal has a solid positive correlation with Fe^T ($R^2 = 0.84$) (Fig. 4a), while pyrite is present in some samples (Table 2). CaO and MnO have a strong positive correlation between themselves ($R^2 = 0.98$) (Fig. 4b), and both are highly correlated with Fe^T and S (0.86–0.98) (Table 4), implying that Mn in coal is related to calcite, and Ca and Mn in calcite are associated with pyrite.

5.1.2. Modes of occurrence of major elements in oil shale

SiO_2, Al_2O_3, K_2O and TiO_2 in oil shale are relatively strongly correlated with ash yield (0.50–0.63) and also each other (Table 6). This suggests their origin from a mixed clay assemblage, similarly to coal. Oil shale samples have relatively low ratios of Al_2O_3/SiO_2, below 0.40 (Table 5), indicating the presence of quartz in addition to clay minerals. This result complies with the amount of quartz contained in oil shale samples (Table 2). Unlike coal, TiO_2 in oil shale has a negative correlation with TOC (–0.26), suggesting that Ti in oil shale is only associated with clastic minerals and has no affinity for organic matter.

Na_2O in oil shale has a strong positive correlation with SiO_2, Al_2O_3, K_2O and TiO_2 (0.72–0.87; Table 6), indicating that clay minerals are responsible for the generation of Na. The content of Na_2O in oil shale (average 0.47 wt%) is higher than in coal (average 0.16 wt%) (Table 5), which proves that besides clay minerals, also plagioclase (Table 2) contributes to the abundance of Na.

The CaO content in oil shale (average 12.51 wt%) is much higher than in coal (average 0.96 wt%) (Table 5), and the contribution of dolomite, aragonite and plagioclase to the presence of Ca in oil shale cannot be ignored (Table 2). Ca is considered to occur in not just one form and it can be present in carbonate and organic associations [36, 51]. The positive correlation between CaO and MgO (0.42) (Fig. 4c) in oil shale indicates the contribution of dolomite. It is worth noting that Ca-bearing fossils such as bivalves and ostracods are present in the Yuqia oil shale in high amounts [27] and are responsible for the abundance of Ca in oil shale samples.

Fe^T in oil shale exhibits no relationship with total sulfur, but has a relatively strong positive correlation with ash yield (0.55), which demonstrates the

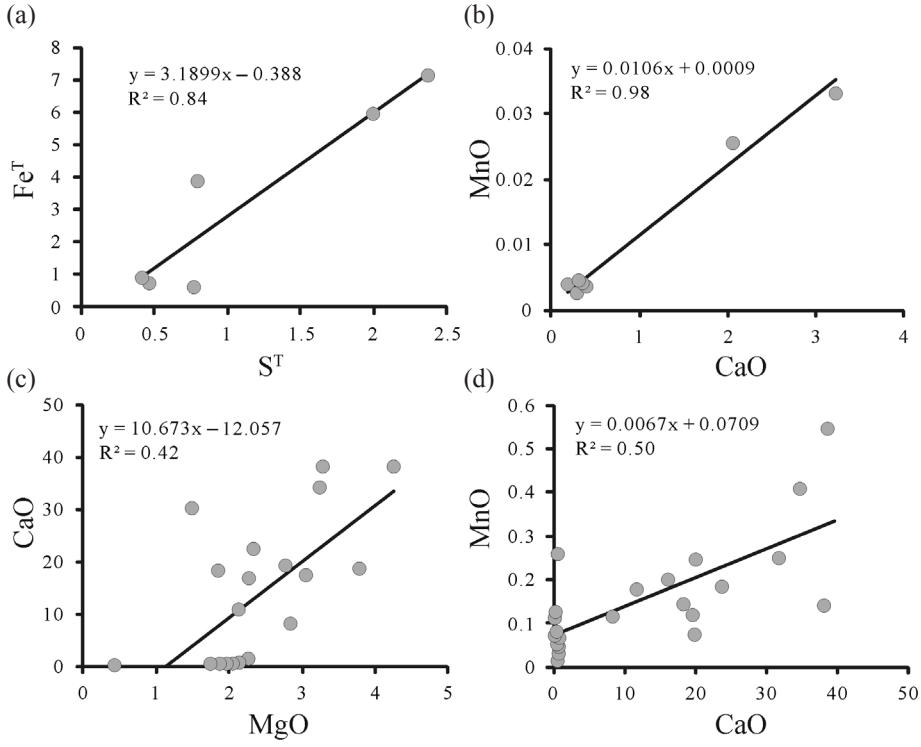

Fig. 4. Correlation diagrams of selected elements in coal and oil shale samples.

affinity of Fe for clay minerals besides siderite. MnO in oil shale has a positive correlation with Fe^T (0.35) and CaO (0.50) (Fig. 4d), suggesting that Mn in oil shale is associated with carbonate minerals. P_2O_5 in oil shale has a relatively strong positive correlation with CaO (0.71) and MnO (0.43), which gives evidence of the important role of carbonate minerals in the rich generation of P.

5.2. Affinities of trace elements

5.2.1. Affinities of trace elements in coal

In the Yuqia coal, the elements Li, Sc, V, Ni, Ga, Rb, In, Sb, Cs, Nb, Ta, Zr and Hf are strongly correlated with ash yield (≥ 0.55; Table 4), indicating the prevailingly inorganic affinities of these elements. All of these elements, except Sc, have a good correlation with SiO_2, Al_2O_3, MgO, Na_2O, K_2O and Ti_2O (≥ 0.60; Table 4), suggesting their association also with clay minerals in coal. It should be noted that Li, Rb, Cs, Nb, Ta, and Hf are also positively correlated with TOC (≥ 0.54), which points towards a certain degree of organic affinity of these elements.

Cr, Pb and Bi show a relatively weak correlation with ash yield (0.30, 0.31 and 0.11, respectively; Table 4). At the same time, their correlation coefficients with TOC are relatively high (0.44, 0.41 and 0.40, respectively),

Table 5. Major component concentrations in Yuqia coal and oil shale

Sample No.	Lithology	SiO_2, wt%	Al_2O_3, wt%	Fe^T, wt%	MgO, wt%	CaO, wt%	Na_2O, wt%	K_2O, wt%	MnO, wt%	Ti_2O, wt%	P_2O_5, wt%	LOI, wt%	FeO, wt%	Al_2O_3/SiO_2	CIA
YY-1	Coal	28.42	15.00	0.75	0.48	0.39	0.23	1.04	0.004	0.50	0.04	52.54	0.62	0.53	88.80
YY-2	Coal	1.44	1.19	0.34	0.13	0.30	0.10	0.04	0.003	0.04	0.11	96.16	0.22	0.83	76.92
YY-3	Coal	12.75	6.75	0.98	0.29	0.31	0.18	0.44	0.004	0.25	0.15	77.56	0.37	0.53	87.33
YY-4	Coal	3.12	1.87	4.05	0.17	0.19	0.15	0.14	0.004	0.05	0.13	89.99	0.16	0.60	81.89
YY-5	Coal	8.11	6.12	6.02	0.22	2.01	0.14	0.20	0.026	0.12	0.21	76.65	0.25	0.75	90.03
YY-6	Coal	3.72	1.79	7.12	0.18	3.22	0.14	0.13	0.033	0.08	0.09	83.46	0.17	0.48	74.67
YY-7	Coal	8.90	3.94	0.46	0.25	0.34	0.18	0.28	0.004	0.19	0.08	84.98	0.10	0.44	81.79
Average		9.49	5.24	2.82	0.25	0.96	0.16	0.32	0.011	0.18	0.12	80.19	0.27	0.59	83.06
YY-8	Oil shale	47.11	28.42	1.36	0.33	0.16	0.15	1.16	0.005	0.97	0.04	19.83	0.29	0.60	94.36
YY-9	Oil shale	53.77	20.88	4.47	1.84	0.35	0.50	2.62	0.127	0.78	0.10	14.36	2.18	0.39	83.68
YY-10	Oil shale	53.89	19.33	4.97	1.92	0.39	0.58	2.69	0.077	0.72	0.11	15.10	3.74	0.36	81.73
YY-11	Oil shale	53.85	19.17	4.71	1.84	0.54	0.62	2.45	0.131	0.72	0.10	15.75	3.33	0.36	81.27
YY-12	Oil shale	53.39	18.53	6.17	1.91	0.48	0.67	2.47	0.269	0.68	0.10	15.04	4.54	0.35	80.76
YY-13	Oil shale	54.95	18.89	4.26	1.95	0.54	0.63	2.39	0.061	0.65	0.09	15.43	1.95	0.34	81.17
YY-14	Oil shale	24.13	7.92	6.05	4.25	39.62	0.26	1.11	0.562	0.32	1.35	14.32	0.19	0.33	79.36
YY-15	Oil shale	51.78	17.82	4.56	1.90	0.49	0.68	2.24	0.034	0.66	0.09	19.48	1.80	0.34	80.83
YY-16	Oil shale	49.64	14.92	4.27	1.87	0.79	0.80	2.04	0.071	0.62	0.29	24.24	2.04	0.30	77.72
YY-17	Oil shale	51.52	17.18	4.62	2.05	0.67	0.74	2.35	0.052	0.71	0.17	19.68	3.56	0.33	78.89
YY-18	Oil shale	20.02	5.75	5.26	3.25	35.62	0.23	0.75	0.426	0.24	0.98	27.22	0.35	0.29	78.55
YY-19	Oil shale	41.44	10.65	4.18	2.16	11.70	0.53	1.36	0.187	0.41	0.46	26.33	2.00	0.26	76.84
YY-20	Oil shale	54.14	17.14	4.33	2.26	0.80	0.80	2.52	0.031	0.70	0.15	17.05	1.87	0.32	76.90
YY-21	Oil shale	21.10	4.99	3.73	1.49	31.73	0.36	0.73	0.249	0.20	1.59	33.30	2.66	0.24	71.81
YY-22	Oil shale	25.13	8.48	3.75	2.34	23.74	0.35	1.07	0.175	0.30	0.50	33.60	1.52	0.34	78.69
YY-23	Oil shale	29.18	9.30	5.36	1.85	19.57	0.44	1.22	0.120	0.35	0.74	31.29	1.45	0.32	77.10
YY-24	Oil shale	26.62	7.58	2.63	3.84	19.47	0.44	1.12	0.068	0.29	0.17	37.46	1.95	0.28	74.10
YY-25	Oil shale	22.31	4.06	3.89	3.28	38.11	0.33	0.51	0.132	0.19	0.56	26.60	1.03	0.18	71.24
YY-26	Oil shale	37.17	12.99	6.42	2.84	8.29	0.42	1.63	0.117	0.42	0.22	28.90	4.42	0.35	80.53
YY-27	Oil shale	49.87	14.95	4.15	1.69	0.81	0.75	2.02	0.069	0.59	0.27	22.80	2.07	0.30	77.85
YY-28	Oil shale	29.25	10.81	5.41	2.26	18.23	0.32	1.35	0.145	0.32	0.17	31.13	4.06	0.37	81.09
YY-29	Oil shale	24.70	9.96	5.60	3.04	16.08	0.26	1.21	0.199	0.39	0.20	37.79	3.42	0.40	82.10
YY-30	Oil shale	22.82	9.27	5.87	2.82	19.94	0.25	1.10	0.247	0.36	0.22	36.54	3.49	0.41	82.06
Average		39.03	13.43	4.61	2.30	12.53	0.48	1.66	0.155	0.50	0.38	24.49	2.34	0.34	79.51

Note: LOI denotes loss on ignition.

and with SiO_2, Al_2O_3, MgO, Na_2O, K_2O and Ti_2O high (0.60–0.86; Table 4), giving evidence of their significant contribution to clay mineral affinities. Co, Sr, Ba and Tl have a high positive correlation with total S and Fe^T (0.55–0.72; Table 4), demonstrating their affinities for pyrite present in coal.

5.2.2. Affinities of trace elements in oil shale

In the Yuqia oil shale, the correlation coefficients of Th, Li, Be, Sc, V, Co, Ni, Zn, Ga, Rb, Cd, In, Cs, W, Tl, Pb, Bi, Ta, Zr and Hf with ash yield are all positive and relatively high (R^2 = 0.50–0.73), while those with TOC are negative (R^2 = –0.52 to –0.24) (Table 6), indicating the predominantly inorganic affinities of these elements. Besides, all the above elements are highly correlated with SiO_2, Al_2O_3, Na_2O, K_2O and TiO_2 ($R^2 \geq 0.50$; Table 6), demonstrating the important role of clay minerals in the formation of these elements. Pb also has a positive correlation with Fe^T (0.41; Table 6), suggesting that siderite might have been the carrier of Pb in oil shale.

Cr, Cu, Sb and Nb exhibit a positive correlation with ash yield (0.34–0.45) and a negative correlation with TOC (–0.44 to –0.13) (Table 6). The correlation coefficients of these elements, except Sb, with SiO_2, Al_2O_3, Na_2O, K_2O and Ti_2O are high (0.57–0.96; Table 6), demonstrating their affinities for clay minerals. Sb has a relatively good correlation with Fe^T (R^2 = 0.47) and Mn (R^2 = 0.33). As discussed above, the amount of Mn in oil shale is controlled by calcium carbonate and siderite, but Sb shows no correlation with CaO (R^2 = 0.01), thus, we can conclude that the Sb amount in oil shale is mainly controlled by siderite. Mo has a positive correlation with both CaO (R^2 = 0.32) and P_2O_5 (R^2 = 0.71), proving the affinity of P for carbonate minerals and its possible presence mainly in carbonate minerals.

5.3. Affinities of REEs

REEs in coal and oil shale have different characteristics. In coal, ΣREE is highly correlated with P_2O_5 (R^2 = 0.72) and MnO (R^2 = 0.42), suggesting the possible occurrence of REEs in phosphate minerals. ΣREE in coal also correlates positively with total sulfur (0.49), Fe^T (0.43) and MnO (0.42) as well as Sr (0.98) and Ba (0.97) (Table 4). As demonstrated above, Ca, Mn, Sr and Ba in coal are all associated with pyrite and have exhibited the affinities of REEs with pyrite in coal.

ΣREE in oil shale has a negative correlation with TOC (R^2 = –0.43), but a positive correlation with ash yield (R^2 = 0.82), SiO_2 (R^2 = 0.74), Al_2O_3 (R^2 = 0.83), Na_2O (R^2 = 0.42), K_2O (R^2 = 0.78) and Ti_2O (R^2 = 0.81) (Table 6). This gives evidence of inorganic affinities of REEs in oil shale and their association primarily with clay minerals and quartz.

REEs typically originate from seawater and terrigenous substances [2]. The chondrite-normalized Ce anomaly (Ce_N/Ce_N^*) is often used as a signature

Table 6. The correlation coefficients (R^2) between ΣREE, total sulfur, TOC, and major and rare earth elements of Yuqia oil shale

	TOC	S^T	Ash	SiO_2	Al_2O_3	Fe^T	MgO	CaO	Na_2O	K_2O	MnO	Ti_2O	P_2O_5	ΣREE	Th	U	Li	Be	Sc	V
TOC	1.00	□	□	□	□	□	□	□	□	□	□	□	□	□	□	□	□	□	□	□
S^T	–0.09	1.00	□	□	□	□	□	□	□	□	□	□	□	□	□	□	□	□	□	□
Ash	0.12	–0.28	1.00	□	□	□	□	□	□	□	□	□	□	□	□	□	□	□	□	□
SiO_2	–0.29	–0.13	0.50	1.00	□	□	□	□	□	□	□	□	□	□	□	□	□	□	□	□
Al_2O_3	–0.27	–0.29	0.63	0.95	1.00	□	□	□	□	□	□	□	□	□	□	□	□	□	□	□
Fe^T	0.35	–0.01	0.55	0.03	0.19	1.00	□	□	□	□	□	□	□	□	□	□	□	□	□	□
MgO	0.27	–0.02	–0.30	–0.48	–0.42	–0.06	1.00	□	□	□	□	□	□	□	□	□	□	□	□	□
CaO	0.15	0.18	–0.56	–0.96	–0.96	–0.17	0.42	1.00	□	□	□	□	□	□	□	□	□	□	□	□
Na_2O	–0.15	0.01	0.24	0.87	0.72	–0.17	–0.44	–0.82	1.00	□	□	□	□	□	□	□	□	□	□	□
K_2O	–0.25	–0.24	0.51	0.97	0.99	0.12	–0.42	–0.96	0.79	1.00	□	□	□	□	□	□	□	□	□	□
MnO	0.11	0.08	0.12	–0.52	–0.46	0.35	–0.01	0.50	–0.60	–0.50	1.00	□	□	□	□	□	□	□	□	□
Ti_2O	–0.26	–0.24	0.53	0.96	0.98	0.11	–0.43	–0.96	0.80	0.98	–0.48	1.00	□	□	□	□	□	□	□	□
P_2O_5	0.00	0.18	–0.47	–0.55	–0.66	–0.25	–0.30	0.71	–0.34	–0.62	0.43	–0.61	1.00	□	□	□	□	□	□	□
ΣREE	–0.43	–0.35	0.82	0.74	0.83	0.10	–0.41	–0.72	0.42	0.78	–0.20	0.81	–0.52	1.00	□	□	□	□	□	□
Th	–0.38	–0.27	0.61	0.79	0.89	0.16	–0.32	–0.80	0.50	0.86	–0.27	0.89	–0.61	0.94	1.00	□	□	□	□	□
U	–0.28	–0.12	0.12	0.17	0.27	0.09	–0.16	–0.16	–0.11	0.20	0.19	0.27	–0.07	0.50	0.53	1.00	□	□	□	□
Li	–0.30	–0.34	0.70	0.88	0.95	0.19	–0.37	–0.89	0.61	0.93	–0.31	0.95	–0.64	0.92	0.96	0.46	1.00	□	□	□
Be	–0.41	–0.27	0.62	0.90	0.95	0.09	–0.45	–0.86	0.62	0.94	–0.32	0.93	–0.54	0.93	0.95	0.39	0.97	1.00	□	□
Sc	–0.38	–0.26	0.73	0.86	0.93	0.15	–0.43	–0.84	0.56	0.90	–0.28	0.91	–0.59	0.96	0.96	0.47	0.97	0.97	1.00	□
V	–0.47	–0.22	0.51	0.77	0.87	0.11	–0.42	–0.74	0.48	0.84	–0.28	0.85	–0.52	0.92	0.95	0.46	0.91	0.94	0.95	1.00
Cr	–0.28	–0.06	0.45	0.84	0.87	0.09	–0.38	–0.83	0.70	0.88	–0.39	0.91	–0.56	0.81	0.90	0.35	0.90	0.89	0.90	0.90
Co	–0.25	–0.05	0.55	0.71	0.75	0.23	–0.31	–0.74	0.56	0.73	–0.21	0.80	–0.53	0.80	0.89	0.45	0.85	0.79	0.85	0.84
Ni	–0.33	–0.11	0.59	0.70	0.74	0.25	–0.49	–0.66	0.49	0.72	–0.03	0.76	–0.35	0.86	0.89	0.48	0.84	0.84	0.88	0.88
Cu	–0.44	–0.07	0.37	0.76	0.81	0.05	–0.28	–0.75	0.57	0.82	–0.37	0.85	–0.56	0.84	0.95	0.45	0.88	0.88	0.89	0.93
Zn	–0.36	–0.21	0.58	0.90	0.95	0.14	–0.36	–0.88	0.62	0.93	–0.38	0.94	–0.62	0.90	0.96	0.46	0.98	0.97	0.96	0.94
Ga	–0.36	–0.23	0.57	0.89	0.95	0.16	–0.39	–0.87	0.62	0.94	–0.36	0.94	–0.62	0.89	0.96	0.41	0.98	0.98	0.97	0.96
Rb	–0.32	–0.22	0.50	0.95	0.97	0.09	–0.42	–0.92	0.76	0.98	–0.45	0.97	–0.60	0.82	0.90	0.28	0.95	0.96	0.93	0.90
Sr	0.06	0.15	–0.36	–0.69	–0.72	–0.18	0.31	0.70	–0.50	–0.70	0.20	–0.69	0.52	–0.47	–0.52	–0.20	–0.67	–0.64	–0.58	–0.51
Mo	–0.18	–0.01	–0.22	–0.21	–0.29	–0.12	–0.35	0.32	–0.04	–0.28	0.07	–0.25	0.71	–0.20	–0.23	0.07	–0.27	–0.24	–0.28	–0.17
Cd	–0.52	–0.26	0.58	0.73	0.82	0.09	–0.37	–0.70	0.40	0.78	–0.19	0.81	–0.48	0.96	0.97	0.60	0.92	0.93	0.94	0.96
In	–0.39	–0.19	0.53	0.85	0.92	0.10	–0.35	–0.83	0.57	0.89	–0.36	0.89	–0.62	0.87	0.95	0.45	0.95	0.95	0.95	0.95
Sb	–0.13	–0.14	0.34	0.01	0.14	0.47	–0.37	0.01	–0.16	0.09	0.33	0.10	0.11	0.37	0.30	0.32	0.20	0.20	0.30	0.36
Cs	–0.35	–0.34	0.62	0.90	0.96	0.15	–0.41	–0.87	0.62	0.95	–0.34	0.92	–0.61	0.87	0.92	0.36	0.95	0.96	0.95	0.91
Ba	–0.27	0.04	0.13	0.38	0.30	–0.15	–0.20	–0.32	0.46	0.35	–0.29	0.40	–0.07	0.45	0.48	0.18	0.39	0.39	0.43	0.44
W	–0.35	–0.31	0.57	0.89	0.93	0.10	–0.44	–0.86	0.69	0.93	–0.33	0.93	–0.57	0.86	0.93	0.37	0.95	0.94	0.93	0.90
Tl	–0.37	–0.40	0.50	0.38	0.48	0.33	–0.38	–0.34	0.17	0.45	0.26	0.48	–0.14	0.58	0.58	0.29	0.60	0.57	0.52	0.50
Pb	–0.24	–0.29	0.65	0.47	0.66	0.41	–0.14	–0.55	0.16	0.60	–0.03	0.64	–0.58	0.82	0.89	0.56	0.79	0.72	0.79	0.82
Bi	–0.24	–0.28	0.63	0.43	0.63	0.36	–0.05	–0.51	0.10	0.56	–0.08	0.59	–0.63	0.79	0.86	0.53	0.75	0.69	0.76	0.81
Nb	–0.33	–0.14	0.45	0.90	0.93	0.12	–0.38	–0.89	0.71	0.94	–0.37	0.96	–0.60	0.84	0.94	0.37	0.96	0.95	0.93	0.92
Ta	–0.28	–0.18	0.50	0.87	0.92	0.19	–0.37	–0.86	0.65	0.92	–0.30	0.94	–0.60	0.84	0.95	0.43	0.97	0.94	0.93	0.91
Zr	–0.36	–0.11	0.61	0.86	0.92	0.27	–0.42	–0.83	0.57	0.91	–0.22	0.90	–0.58	0.88	0.95	0.44	0.94	0.96	0.95	0.92
Hf	–0.45	–0.07	0.51	0.88	0.92	0.13	–0.39	–0.86	0.61	0.91	–0.36	0.90	–0.59	0.86	0.92	0.36	0.92	0.96	0.94	0.94

Note: Fe^T represents total Fe.

Continuation of Table 6.

Cr	Co	Ni	Cu	Zn	Ga	Rb	Sr	Mo	Cd	In	Sb	Cs	Ba	W	Tl	Pb	Bi	Nb	Ta	Zr	Hf
□	□	□	□	□	□	□	□	□	□	□	□	□	□	□	□	□	□	□	□	□	□
□	□	□	□	□	□	□	□	□	□	□	□	□	□	□	□	□	□	□	□	□	□
□	□	□	□	□	□	□	□	□	□	□	□	□	□	□	□	□	□	□	□	□	□
□	□	□	□	□	□	□	□	□	□	□	□	□	□	□	□	□	□	□	□	□	□
□	□	□	□	□	□	□	□	□	□	□	□	□	□	□	□	□	□	□	□	□	□
□	□	□	□	□	□	□	□	□	□	□	□	□	□	□	□	□	□	□	□	□	□
□	□	□	□	□	□	□	□	□	□	□	□	□	□	□	□	□	□	□	□	□	□
□	□	□	□	□	□	□	□	□	□	□	□	□	□	□	□	□	□	□	□	□	□
□	□	□	□	□	□	□	□	□	□	□	□	□	□	□	□	□	□	□	□	□	□
□	□	□	□	□	□	□	□	□	□	□	□	□	□	□	□	□	□	□	□	□	□
□	□	□	□	□	□	□	□	□	□	□	□	□	□	□	□	□	□	□	□	□	□
□	□	□	□	□	□	□	□	□	□	□	□	□	□	□	□	□	□	□	□	□	□
□	□	□	□	□	□	□	□	□	□	□	□	□	□	□	□	□	□	□	□	□	□
□	□	□	□	□	□	□	□	□	□	□	□	□	□	□	□	□	□	□	□	□	□
□	□	□	□	□	□	□	□	□	□	□	□	□	□	□	□	□	□	□	□	□	□
□	□	□	□	□	□	□	□	□	□	□	□	□	□	□	□	□	□	□	□	□	□
□	□	□	□	□	□	□	□	□	□	□	□	□	□	□	□	□	□	□	□	□	□
□	□	□	□	□	□	□	□	□	□	□	□	□	□	□	□	□	□	□	□	□	□
□	□	□	□	□	□	□	□	□	□	□	□	□	□	□	□	□	□	□	□	□	□
□	□	□	□	□	□	□	□	□	□	□	□	□	□	□	□	□	□	□	□	□	□
1.00	□	□	□	□	□	□	□	□	□	□	□	□	□	□	□	□	□	□	□	□	□
0.90	1.00	□	□	□	□	□	□	□	□	□	□	□	□	□	□	□	□	□	□	□	□
0.86	0.93	1.00	□	□	□	□	□	□	□	□	□	□	□	□	□	□	□	□	□	□	□
0.95	0.91	0.88	1.00	□	□	□	□	□	□	□	□	□	□	□	□	□	□	□	□	□	□
0.93	0.84	0.84	0.92	1.00	□	□	□	□	□	□	□	□	□	□	□	□	□	□	□	□	□
0.93	0.85	0.86	0.93	0.99	1.00	□	□	□	□	□	□	□	□	□	□	□	□	□	□	□	□
0.93	0.79	0.80	0.88	0.97	0.97	1.00	□	□	□	□	□	□	□	□	□	□	□	□	□	□	□
–0.57	–0.38	–0.33	–0.42	–0.64	–0.63	–0.67	1.00	□	□	□	□	□	□	□	□	□	□	□	□	□	□
–0.20	–0.08	0.02	–0.14	–0.24	–0.24	–0.23	0.45	1.00	□	□	□	□	□	□	□	□	□	□	□	□	□
0.84	0.84	0.89	0.92	0.93	0.93	0.85	–0.47	–0.12	1.00	□	□	□	□	□	□	□	□	□	□	□	□
0.92	0.83	0.83	0.93	0.98	0.99	0.95	–0.62	–0.25	0.93	1.00	□	□	□	□	□	□	□	□	□	□	□
0.20	0.35	0.51	0.24	0.17	0.21	0.12	0.18	0.31	0.34	0.15	1.00	□	□	□	□	□	□	□	□	□	□
0.85	0.74	0.79	0.84	0.96	0.97	0.97	–0.65	–0.27	0.88	0.95	0.21	1.00	□	□	□	□	□	□	□	□	□
0.56	0.64	0.64	0.62	0.43	0.42	0.42	0.31	0.32	0.46	0.40	0.32	0.34	1.00	□	□	□	□	□	□	□	□
0.90	0.82	0.84	0.87	0.94	0.95	0.96	–0.62	–0.18	0.87	0.91	0.27	0.96	0.46	1.00	□	□	□	□	□	□	□
0.44	0.45	0.56	0.46	0.52	0.53	0.49	–0.37	0.04	0.59	0.47	0.29	0.54	0.19	0.57	1.00	□	□	□	□	□	□
0.72	0.84	0.82	0.82	0.76	0.77	0.65	–0.29	–0.19	0.85	0.76	0.52	0.71	0.43	0.73	0.58	1.00	□	□	□	□	□
0.70	0.78	0.76	0.81	0.74	0.76	0.63	–0.30	–0.24	0.84	0.77	0.44	0.68	0.37	0.67	0.51	0.97	1.00	□	□	□	□
0.97	0.88	0.86	0.94	0.97	0.98	0.97	–0.64	–0.23	0.88	0.95	0.16	0.92	0.48	0.95	0.52	0.74	0.70	1.00	□	□	□
0.95	0.88	0.86	0.91	0.96	0.97	0.95	–0.64	–0.25	0.88	0.94	0.20	0.92	0.46	0.96	0.57	0.77	0.72	0.99	1.00	□	□
0.90	0.83	0.87	0.90	0.96	0.96	0.94	–0.60	–0.28	0.91	0.93	0.31	0.94	0.42	0.92	0.57	0.78	0.74	0.95	0.95	1.00	□
0.90	0.81	0.83	0.91	0.96	0.97	0.94	–0.60	–0.24	0.91	0.96	0.18	0.93	0.40	0.88	0.45	0.71	0.71	0.94	0.90	0.95	1.00

of seawater, and both LREEs and HREEs are enriched in seawater [61]. This shows that both coal and oil shale have negligible chondrite-normalized Ce anomalies and display similar traits of LREE enrichment and HREE deficit (Table 3; Fig. 3), which excludes seawater as a source of REEs. As a whole, similar vertical trends of ΣREE, ΣLREE and ΣHREE are exposed (Fig. 2), which points to the same controlling factors of REEs in coal and oil shale. In addition, the Yuqia coal and oil shale also reveal similar normalized distribution patterns (Fig. 3), which provides good evidence for the same REE origin and formation process of these rocks [62, 63]. The chondrite-normalized curves of coal and oil shale have a negative Eu anomaly, which is likely inherited from their source rocks [64, 65], implying that REEs in both coal and oil shale originate from terrigenous substances. Moreover, ΣREE in oil shale has a good positive correlation with terrigenous elements Th ($R^2 = 0.94$), Li ($R^2 = 0.92$), Be ($R^2 = 0.93$), Sc ($R^2 = 0.96$), V ($R^2 = 0.92$) and Zn ($R^2 = 0.90$), but a negative correlation with some typical non–terrigenous elements such as Sr ($R^2 = –0.47$). This may be a sign of the terrigenous origin of REEs in oil shale, while in coal, they have no significant positive correlation with terrigenous trace elements.

5.4. Weathering and provenance

5.4.1. Source area weathering

The chemical index of alteration (CIA) reflects the weathering degree of rocks and paleoclimate and is calculated using the molecular proportions of the following compounds: $CIA = [Al_2O_3/(Al_2O_3 + CaO^* + Na_2O + K_2O)] \times 100$, where CaO^* is the amount of CaO incorporated in the silicate fraction of the rock, while the molecular proportions are calculated by dividing the amount of the compounds by their relative atomic mass. The CIA value of 50–65 indicates a cold and dry climate during low chemical weathering, CIA of 65–85 is indicative of a warm and humid climate during moderate chemical weathering, whereas its value between 85 and 100 signifies a hot and humid climate during strong chemical weathering [66, 67]. The average value of CIA for coal is 83.06 and for oil shale 79.51 (Table 5). These figures demonstrate that both coal and oil shale in the Yuqia area are possibly the products of source rocks that have experienced moderate chemical weathering during a warm and humid climate.

The Al_2O_3 vs ($Na_2O + CaO^*$) vs K_2O (A-CN-K) ternary plot is also used to deduce chemical weathering trends [66, 69, 70]. Both coal and oil shale have displayed distribution trends that are approximately parallel to the A-CN axis; with the increase of the value of CIA, coal and oil shale tend to be distributed closer to the A-K axis (Fig. 5a). All the samples are located within the area of illite and kaolinite-chlorite. This aluminum-rich composition results from enhanced chemical weathering [70–72], while the finding is in agreement with

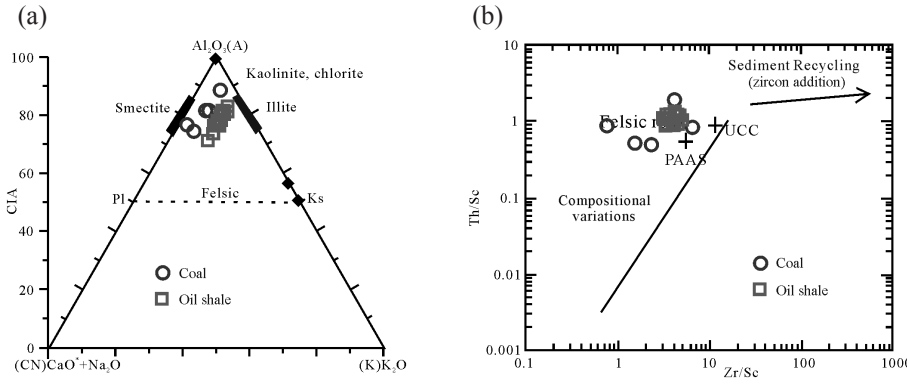

Fig. 5. A-CN-K and Zr/Sc-Th/Sc diagrams for coal and oil shale samples (base map sources: a) [66]; b) [67]).

the XRD results for tested clay minerals (Table 2). The Yuqia coal and oil shale are closely and densely distributed (Fig. 5a), suggesting their uniform weathering process.

5.4.2. Provenance and source of REEs

The depositional process such as mineral sorting might change the abundance of some minerals, thus causing the enrichment of specific elements [73]. The ratio of Th/Sc has remained stable during the sediment recycling process [68], and Zr/Sc has not been influenced by the later hydrothermal alteration [74], so, both can be used to reflect the compositional changes, mineral sorting and heavy mineral content of source rocks [68]. Most samples are plotted in the diagram of Zr/Sc vs Th/Sc close to PAAS and UCC (Fig. 5b), indicating that the component contents of the samples are controlled by the source rocks. Both coal and oil shale are distributed above the line of compositional variations (Fig. 5b), suggesting their generation from felsic source rocks. The diagrams of La/Th vs Hf, Th/Sc vs La/Sc and La/Yb vs ΣREE can mirror the source rocks of sedimentary rocks [75–78]. The samples have a mixed provenance of felsic and basic volcanic rocks and felsic sedimentary rocks (Fig. 6).

The REE abundance can also be used to infer the source of sedimentary rocks [68, 73, 79]. Commonly, felsic source rocks have relatively high ratios of LREE/HREE and negative Eu anomalies when normalized to chondritic meteorites, whereas mafic source rocks display relatively low LREE/HREE ratios and no Eu anomalies [44, 73, 80]. At the same time, the chondrite-normalized patterns and parameters indicate that both coal and oil shale samples are characterized by LREE enrichment and HREE deficit.

The geochemical composition within the sediment-source region is one of the important factors controlling the Ce and Eu anomalies [18, 81–84].

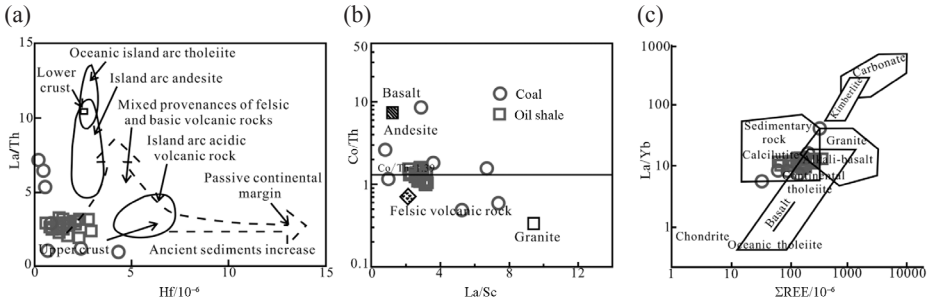

Fig. 6. Diagrams of source rocks (base map sources: a) [77]; b) [75]; c) [78]).

Sediment source regions dominated by felsic or felsic-intermediate rocks are characterized by weakly negative Ce and negative Eu anomalies [64, 65]. The weak negative Ce anomalies may also be caused by oxidation and in-situ precipitation of Ce^{4+} during weathering in the sediment-source region [18]. In the latter region, felsic terrigenous input has sometimes a lower $(La/Lu)_N$ ratio compared to sedimentary terrigenous source regions [18, 85]. The strongly negative Eu (average 0.60) (Table 3) and weakly negative Ce anomalies (average 0.94) (Table 3) of coal indicate the felsic or felsic-intermediate source rocks mixed with sedimentary rocks. Oil shale has weakly negative Ce (average 0.96) and Eu anomalies (average 0.67) (Table 3) and relatively high $(La/Lu)_N$ ratios (average 8.55), suggesting the pronounced sediment terrigenous input differently from coal. Summarizing the above results, we infer that the Yuqia coal and oil shale have similar source rocks of felsic volcanic and sedimentary rocks.

6. Conclusions

1. This study discussed and compared the inorganic geochemistry, provenance and tectonic setting of oil shale and coal in the Yuqia area of the Qaidam Basin, China. Coal is mainly represented by lignite and bituminous coal, and oil shale mostly belongs to medium-quality oil shales. In the chondrite-normalized patterns, both coal and oil shale exhibit LREE enrichment and HREE deficit with negative Eu and negligible Ce anomalies.

2. In both coal and oil shale, Si, Al, K, Ti and Na originate from a mixed clastic sedimentary component comprised of clay minerals, quartz and feldspars. In coal, Mg is mainly correlated with illite and an illite-smectite mixed layer, Ti is correlated with organic matter and clay minerals, Fe is mainly present in pyrite, Mn is related to calcite, and Ca and Mn are associated with pyrite. Trace elements Li, Rb, Cs, Nb, Ta and Hf are associated with

both organic matter and clay minerals and Co, Sr, Ba and Tl have strong affinities for pyrite. In oil shale, Ti has only an inorganic affinity, whereas Na has another source, potentially plagioclase. Mn is associated with carbonate minerals, P is related to carbonate minerals and Ca is associated with carbonate minerals and Ca-bearing fossils. Most trace elements are related to clay minerals. Li, Co, Ni, Ga, Cs, Pb, Bi and Ta might also have the carrier of siderite; Cr, Cu and Nb have clay-mineral affinities; Sb is mainly controlled by siderite, but Mo has good affinities for carbonate minerals.

3. In coal, REEs are related to phosphate minerals, while REEs in oil shale have inorganic affinities and are mainly associated with clay minerals and quartz. The REEs in coal and oil shale are of terrigenous origin. Coal and oil shale are possibly the products of source rocks that have experienced moderate chemical weathering during a warm and humid climate; they both have similar source rocks of felsic volcanic and sedimentary rocks.

Acknowledgments

Borehole YYY-1 was generously provided by the China Geological Survey. The research project was financially supported by the project "Geological survey and evaluation of oil shales in China (No. DD20189607)", the project No. 2018M631540 supported by the China Postdoctoral Science Foundation and "Potential evaluation of oil shale in the Yuqia area, Qaidam Basin (No. DDYZ20150012)". Many thanks are conveyed to Professor Shifeng Dai and two anonymous reviewers for their constructive comments to improve the manuscript.

REFERENCES

1. Wang, P. L., Li, Z. X., Lv, D. W., Wang, Z. F., Liu, H. Y., Wang, D. D., Feng, T. T. Analysis on palaeoclimate and metallogenic materials of typical basins under co-occurring circumstances of coal and oil shale. *Coal Geology of China*, 2013, **25**(12), 8–11 (in Chinese).
2. Bai, Y. Y., Liu, Z. J., Sun, P. C., Hu, X. F., Zhao, H. Q. Rare earth and major element geochemistry of Eocene fine-grained sediments in oil shale- and coal-bearing layers of the Meihe Basin, Northeast China. *J. Asian Earth Sci.*, 2015, **97**(Part A), 89–101.
3. Xu, S. C., Liu, Z. J., Dong, Q. S., Liu, S. Y., Liu, R., Meng, Q. T. Eocene sedimentary evolution and its control over coal & oil shale development in Fushun Coalfield. *Journal of China University of Petroleum*, 2012, **36**(2), 45–52 (in Chinese).

4. Bai, Y. L., Ma, L., Wu, W. J., Ma, Y. H. Geological characteristics and resource potential of oil shale in Ordos basin. *Geology in China*, 2009, **36**(5), 1123–1137 (in Chinese).
5. Wang, B. S., Yu, J. F., Sun, Y. Z., Li, M. Y. Analysis on peat swamp types from Huangxian Tertiary brown coal and oil shale bearing basin. *Coal Geology & Exploration*, 2001, **29**(5), 1–3 (in Chinese).
6. Gibling, M. R., Srisuk, S., Ulkakimaphan, Y. Oil shale and coal in intermontane basins of Thailand. *AAPG Bull.*, 1985, **69**(5), 760–766.
7. Xu, S. C., Liu, Z. J., Dong, Q. S., Chen, H. J., Liu, R. Deposition and sedimentary evolution of coal, oil shale and evaporite-bearing strata in terrestrial basins. *Journal of Jilin University (Earth Science Edition)*, 2012, **42**(2), 296–303 (in Chinese).
8. Sun, P. C., Sachsenhofer, R. F., Liu, Z. J., Strobl, S. A. I., Meng, Q. T., Liu, R., Zhen, Z. Organic matter accumulation in the oil shale- and coal-bearing Huadian Basin (Eocene; NE China). *Int. J. Coal Geol.*, 2013, **105**, 1–15.
9. Ward, C. R. Analysis and significance of mineral matter in coal seams. *Int. J. Coal Geol.*, 2000, **50**(1–4), 135–168.
10. Gürdal, G. Geochemistry of trace elements in Çan coal (Miocene), Çanakkale, Turkey. *Int. J. Coal Geol.*, 2008, **74**(1), 28–40.
11. Finkelman, R. B. The use of modes of occurrence information to predict the removal of the hazardous air pollutants prior to combustion. *J. Coal Qual.*, 1993, **12**(4), 132–134.
12. Finkelman, R. B. Modes of occurrence of environmentally-sensitive trace elements of coal. In: *Environmental Aspects of Trace Elements in Coal* (Swaine, D. J., Goodarzi, F., eds.). Kluwer Academic Publishers, the Netherlands, 1995, 24–50.
13. Swaine, D. J. Why trace elements are important. *Fuel Process. Technol.*, 2000, **65**–**66**, 21–33.
14. Xu, M., Yan, R., Zheng, C., Qiao, Y., Han, J., Sheng, C. Status of trace element emission in a coal combustion process: a review. *Fuel Process. Technol.*, 2004, **85**(2–3), 215–237.
15. Li, Z. S., Ward, C. R., Gurba, L. W. Occurrence of non-mineral inorganic elements in macerals of low-rank coals. *Int. J. Coal Geol.*, 2010, **81**(4), 242–250.
16. Dai, S. F., Liu, J. J., Ward, C. R., Hower, J. C., Xie, P. P., Jiang, Y. F., Hood, M. M., O'Keefe, J. M. K., Song, H. Petrological, geochemical, and mineralogical compositions of the low-Ge coals from the Shengli coalfield, China: A comparative study with Ge-rich coals and a formation model for coal-hosted Ge ore deposit. *Ore Geol. Rev.*, 2015, **71**, 318–349.
17. Seredin, V. V., Dai, S. F. Coal deposits as potential alternative sources for lanthanides and yttrium. *Int. J. Coal Geol.*, 2012, **94**, 67–93.
18. Dai, S. F., Graham, I. T., Ward, C. R. A review of anomalous rare earth elements and yttrium in coal. *Int. J. Coal Geol.*, 2016, **159**, 82–95.
19. Bhatia, M. R. Rare earth element geochemistry of Australian Paleozoic graywackes and mudrocks: Provenance and tectonic control. *Sediment. Geol.*, 1985, **45**(1–2), 97–113.

20. Wignall, P. B., Myers, K. J. Interpreting benthic oxygen levels in mudrocks: A new approach. *Geology*, 1988, **16**(5), 452–455.
21. Jones, B., Manning, D. A. C. Comparison of geochemical indices used for the interpretation of palaeoredox conditions in ancient mudstones. *Chem. Geol.*, 1994, **111**(1–4), 111–129.
22. McLennan, S. M. Relationships between the trace element composition of sedimentary rocks and upper continental crust. *Geochem. Geophy. Geosy.*, 2001, **2**(4), Paper number 20000GC000109.
23. Tanaka, K., Akagawa, F., Yamamoto, K., Tani, Y., Kawabe, I., Kawai, T. Rare earth element geochemistry of Lake Baikal sediment: its implication for geochemical response to climate change during the Last Glacial/Interglacial transition. *Quaternary Sci. Rev.*, 2007, **26**(9–10), 1362–1368.
24. Yue, T. X. Middle Jurassic series coal-bearing strata characteristic analysis in Lenghu-Iqe area, Qinghai province. *Coal Geology of China*, 2011, **23**(12), 18–20 (in Chinese).
25. Chen, L. *The Study of Sedimentary Characteristics and Accumulation of Iqe Coalfield in Qinghai Province*. Master Thesis, Xi'an University of Science and Technology, 2013 (in Chinese).
26. Zhao, P. A study on physical property of oil shale on north margin of Qaidam basin, Qinghai province. *Coal Geology of China*, 2011, **23**(12), 39–41 (in Chinese).
27. Ma, X. M., Hao, H. Y., Ma, F., Duan, G. L., Cheng, Y. H. Developmental value of oil shale in the 7th Member of Middle Jurassic in Yuqia Area, Qaidam Basin. *Journal of Southwest Petroleum University (Science & Technology Edition)*, 2013, **35**(3), 52–59.
28. Liu, Z. J., Yang, H. L., Dong, Q. S., Zhu, J. W., Guo, W., Ye, S. Q., Liu, R., Meng, Q. T., Zhang, H. L., Gan, S. C. *Oil Shale in China*. Petroleum Industry Press, 2008, 14–28 (in Chinese with English abstract).
29. GB/T 19145-2003. *Determination of Total Organic Carbon in Sedimentary Rock*, 2003 (in Chinese).
30. ASTM D3177-02. *Standard Test Methods for Total Sulfur in the Analysis Sample of Coal and Coke*. ASTM International, West Conshohocken, PA, 2007.
31. SH/T 0508-92. *The Test Method for Oil Yield from Oil Shale – The Method of Low Temperature Carbonization*, 1992 (in Chinese).
32. ASTM D3173-11. *Standard Test Method for Moisture in the Analysis Sample of Coal and Coke*. ASTM International, West Conshohocken, PA, 2011.
33. ASTM D3175-11. *Standard Test Method for Volatile Matter in the Analysis Sample of Coal and Coke*. ASTM International, West Conshohocken, PA, 2011.
34. ASTM D3174-11. *Standard Test Method for Ash in the Analysis Sample of Coal and Coke from Coal*. ASTM International, West Conshohocken, PA, 2011.
35. ASTM D5865-13. *Standard Test Method for Gross Calorific Value of Coal and Coke*. ASTM International, West Conshohocken, PA, 2013.
36. Kimura, T. Relationships between inorganic elements and minerals in coals from the Ashibetsu district, Ishikari coal field, Japan. *Fuel Process. Technol.*, 1998, **56**(1–2), 1–19.

37. Ward, C. R., Spears, D. A., Booth, C. A., Staton, I., Gurba, L. W. Mineral matter and trace elements in coals of the Gunnedah Basin, New South Wales, Australia. *Int. J. Coal Geol.*, 1999, **40**(4), 281–308.
38. Ward, C. R., Taylor, J. C., Matulis, C. E., Dale, L. S. Quantification of mineral matter in the Argonne Premium Coals using interactive Rietveld-based X-ray diffraction. *Int. J. Coal Geol.*, 2001, **46**(2–4), 67–82.
39. Ruan, C. D., Ward, C. R. Quantitative X-ray powder diffraction analysis of clay minerals in Australian coals using Rietveld methods. *Appl. Clay Sci.*, 2002, **21**(5–6), 227–240.
40. GB/T 5751-2009. *Chinese Coal Classification*. China national standardization management committee, 2009.
41. Dai, S., Ren, D., Chou, C. L., Finkelman, R. B., Seredin, V. V., Zhou, Y. Geochemistry of trace elements in Chinese coals: A review of abundances, genetic types, impacts on human health, and industrial utilization. *Int. J. Coal Geol.*, 2012, **94**, 3–21.
42. Finkelman, R. B. Trace and minor elements in coal. In: *Organic Geochemistry* (Engel, M. H., Macko, S. A., eds.). Plenum Press, New York, NY, 1993, 593–607.
43. Ketris, M. P., Yudovich, Ya. E. Estimations of Clarkes for Carbonaceous biolithes: World averages for trace element contents in black shales and coals. *Int. J. Coal Geol.*, 2009, **78**(2), 135–148.
44. Taylor, S. R., McLennan, S. M. *The Continental Crust: Its Composition and Evolution: An Examination of the Geochemical Record Preserved in Sedimentary Rocks*. Science Press, Beijing, 1985.
45. Boynton, W. V. Cosmochemistry of the rare earth elements: meteorite studies. In: *Rare Earth Element Geochemistry* (Henderson, P., ed.), Elsevier, 1983, 63–114.
46. Fu, X., Wang, J., Zeng, Y., Tan, F., Feng, X. Trace elements in marine oil shale from the Changshe Mountain area, northern Tibet, China. *Energ. Source. Part A*, 2012, **34**(24), 2296–2306.
47. Patterson, J. H., Ramsden, A. R., Dale, L. S., Fardy, J. J. Geochemistry and mineralogical residences of trace elements in oil shales from Julia Creek, Queensland, Australia. *Chem. Geol.*, 1986, **55**(1–2), 1–16.
48. Wang, Z. G., Yu, X. Y., Zhao, Z. H. *The Geochemistry of Rare Earth Elements*. Science Press, Beijing, 1989, 73–150 (in Chinese).
49. Hu, X. F., Liu, Z. J., Liu, R., Sun, P. C., Xu, S. C., Meng, Q. T., Liu, S. Y. Clay mineral and inorganic geochemical characteristics of Eocene Huadian formation in Huadian basin and their paleoenvironment implications. *Journal of China Coal Society*., 2012, **37**(3), 416–423 (in Chinese).
50. Liu, R., Liu, Z. J., Guo, W., Chen, H. J., Hu, X. F., Zhou, R. J. Rare earth element characteristics of Bagemaode oil shale, Inner Mongolia, China. *Geochimica*, 2010, **39**(4), 364–370 (in Chinese).
51. Mukhopadhyay, P. K.,Goodarzi, F.,Crandlemire, A. L.,Gillis, K. S.,MacNeil, D. J., Smith, W. D. Comparison of coal composition and elemental distribution in selected seams of the Sydney and Stellarton Basins, Nova Scotia, Eastern

Canada. *Int. J. Coal Geol.*, 1998, **37**(1–2), 113–141.
52. Fu, X. G., Wang, J., Zeng, Y. H., Tan, F. W., Feng, X. L. REE geochemistry of marine oil shale from the Changshe Mountain area, northern Tibet, China. *Int. J. Coal Geol.*, 2010, **81**(3), 191–199.
53. Fu, X. G., Wang, J., Zeng, Y. H., Tan, F. W., He, J. L. Geochemistry and origin of rare earth elements (REEs) in the Shengli River oil shale, northern Tibet, China. *Geochemistry*, 2011, **71**(1), 21–30.
54. Dorsey, A. E., Kopp, O. C. Distribution of elements and minerals between a coal and its overlying sedimentary rocks in a limnic environment. *Int. J. Coal Geol.*, 1985, **5**(3), 261–274.
55. Glick, D. C., Davis, A. Variability in the inorganic element content of U.S. coals including results of cluster analysis. *Org. Geochem.*, 1987, **11**(5), 331–342.
56. Asuen, G. O. Assessment of major and minor elements in the Northumberland Coalfield, England. *Int. J. Coal Geol.*, 1987, **9**(2), 171–186.
57. Finkelman, R. B. Determination of trace element sites in the Waynesburg coal by SEM analysis of accessory minerals. *Scan. Electron Micros.*, 1978, **1**, 143–148.
58. Finkelman, R. B. Modes of occurrence of trace elements and minerals in coal. *US Geol. Survey Open–File Rep.*, 1982, 221–225.
59. Finkelman, R. B., Stanton, R. W. *Fuel*, 1978, **57**(12), 763–768.
60. Shao, L. Y., Jones, T., Gayer, R., Dai, S. F., Li, S. S., Jiang, Y. F., Zhang, P. F. Petrology and geochemistry of the high-sulphur coals from the Upper Permian carbonate coal measure in the Heshan Coalfield, southern China. *Int. J. Coal Geol.*, 2003, **55**(1), 1–26.
61. Murray, R. W., Bruchholtz ten Brink, M. R., Jones, D. L., Gerlach, D. C., Russ, G. P. III. Rare earth elements as indicators of different marine depositional environments in chert and shale. *Geology*, 1990, **18**(3), 268–271.
62. Shi, J. A., Guo, X. L., Wang, Z., Yan, N. Z., Wang, J. X. Geochemistry of REE in QH1 sediments of Qinghai Lake since Late Holocene and its paleoclimatic significance. *Journal of Lake Sciences.,* 2003, **15**(1), 28–34 (in Chinese).
63. Chen, L., Liu, C. L., Zhuang, C., Che, X. G., Wu, J. Rare earth element records of the lower Paleogene sediments in the Sanshui Basin and their paleoclimate implications. *Acta Sedimentologica Sinica*, 2009, **27**(6), 1155–1162.
64. Eskenazy, G. M. Rare earth elements in a sampled coal from the Pirin deposit, Bulgaria. *Int. J. Coal Geol.*, 1987, **7**(3), 301–314.
65. Birk, D., White, J. C. Rare earth elements in bituminous coals and underclays of the Sydney Basin, Nova Scotia: Element sites, distribution, mineralogy. *Int. J. Coal Geol.*, 1991, **19**(1–4), 219–251.
66. Nesbitt, H. W., Young, G. M. Early Proterozoic climates and plate motions inferred from major element chemistry of lutites. *Nature.*,1982, **299**, 715–717.
67. Bock, B., McLennan, S. M., Hanson, G. N. Geochemistry and provenance of the Middle Ordovician Austin Glen Member (Normanskill Formation) and the Taconian Orogeny in New England. *Sedimentology*, 1998, **45**(4), 635–655.
68. McLennan, S. M., Hemming, S., McDaniel, D. K., Hanson, G. N. Geochemical approaches to sedimentation, provenance, and tectonics. In: *Processes*

Controlling the Composition of Clastic Sediments (Johnsson, M. J., Basu, A., eds.), Geological Society of America Special Papers, 1993, **284**, 21–40.

69. Nesbitt, H. W., Young, G. M., McLennan, S. M., Keays, R. R. Effects of chemical weathering and sorting on the petrogenesis of siliciclastic sediments, with implications for provenance studies. *J. Geol.*, 1996, **104**(5), 525–542.
70. Selvaraj, K., Chen, C. T. A. Moderate chemical weathering of subtropical Taiwan: constraints from solid-phase geochemistry of sediments and sedimentary rocks. *J. Geol.*, 2006, **114**(1), 101–116.
71. Nesbitt, H. W., Young, G. M. Prediction of some weathering trends of plutonic and volcanic rocks based on thermodynamic and kinetic considerations. *Geochim. Cosmochim. Ac.*, 1984, **48**(7), 1523–1534.
72. Nath, B. N., Kunzendorf, H., Plüger, W. L. Influence of provenance, weathering, and sedimentary processes on the elemental ratios of the fine-grained fraction of the bedload sediments from the Vembanad Lake and the adjoining continental shelf, southwest coast of India. *J. Sediment. Res.,* 2000, **70**, 1081–1094.
73. Kasanzu, C., Maboko, M. A., Manya, S. Geochemistry of fine-grained clastic sedimentary rocks of the Neoproterozoic Ikorongo Group, NE Tanzania: Implications for provenance and source rock weathering. *Precambrian Res.*, 2008, **164**(3–4), 201–213.
74. Lambeck, A., Huston, D., Maidment, D., Southgate, P. Sedimentary geochemistry, geochronology and sequence stratigraphy as tools to typecast stratigraphic units and constrain basin evolution in the gold mineralized Palaeoproterozoic Tanami Region, Northern Australia. *Precambrian Res.*, 2008, **166**(1–4), 185–203.
75. Wronkiewicz, D. J., Condie, K. C. Geochemistry of Archean shales from the Witwatersrand Supergroup, South Africa: Source-area weathering and provenance. *Geochim. Cosmochim. Ac.*, 1987, **51**(9), 2401–2416.
76. Long, X., Sun, M., Yuan, C., Xiao, W., Cai, K. Early Paleozoic sedimentary record of the Chinese Altai: Implications for its tectonic evolution. *Sediment. Geol.*, 2008, **208**(3–4), 88–100.
77. Floyd, P. A., Leveridge, B. E. Tectonic environment of the Devonian Gramscatho basin, south Cornwall: framework mode and geochemical evidence from turbiditic sandstones. *J. Geol. Soc. London,* 1987, **144**(4), 531–542.
78. Allegre, C. J., Minster, J. F. Quantitative models of trace element behavior in magmatic processes. *Earth Planet. Sc. Lett.*, 1978, **38**(1), 1–25.
79. Asiedu, D. K., Suzuki, S., Nogami, K., Shibata, T. Geochemistry of Lower Cretaceous sediments, inner zone of southwest Japan: Constraints on provenance and tectonic environment. *Geochem. J.*, 2000, **34**(2), 155–173.
80. Roddaz, M., Viers, J., Brusset, S., Baby, P., Boucayrand, C., Herail, G. Controls on weathering and provenance in the Amazonian foreland basin: Insights from major and trace element geochemistry of Neogene Amazonian sediments. *Chem. Geol.*, 2006, **226**(1–2), 31–65.
81. Dai, S. F., Yang, J. Y., Ward, C. R., Hower, J. C., Liu, H. D., Garrison, T. M., French, D., O'Keefe, J. M. K. Geochemical and mineralogical evidence for a coal–hosted uranium deposit in the Yili Basin, Xinjiang, northwestern China. *Ore Geol. Rev.*, 2015, **70**, 1–30.

82. Göb, S., Loges, A., Nolde, N., Bau, M., Jacob, D. E., Markl, G. Major and trace element compositions (including REE) of mineral, thermal, mine and surface waters in SW Germany and implications for water-rock interaction. *Appl. Geochem.*, 2013, **33**, 127–152.
83. Leybourne, M. I., Goodfellow, W. D., Boyle, D. R., Hall, G. M. Rapid development of negative Ce anomalies in surface waters and contrasting REE patterns in groundwaters associated with Zn-Pb massive sulphide deposits. *Appl. Geochem*., 2000, **15**(6), 695–723.
84. Yossifova, M. G., Eskenazy, G. M., Valčeva, S. P. Petrology, mineralogy, and geochemistry of submarine coals and petrified forest in the Sozopol Bay, Bulgaria. *Int. J. Coal Geol.*, 2011, **87**(3–4), 212–225.
85. Aubert, D., Stille, P., Probst, A. REE fractionation during granite weathering and removal by waters and suspended loads: Sr and Nd isotopic evidence. *Geochim. Cosmochim. Ac.*, 2001, **65**(3), 387–406.

Presented by S. Li
Received November 5, 2018